Journal of Medicinal Chemistry

Article

N-Heterocyclic (4-Phenylpiperazin-1-yl)methanones Derived from Phenoxazine and Phenothiazine as Highly Potent Inhibitors of Tubulin Polymerization

Helge Prinz, Ann-Kathrin Ridder, Kirsten Vogel, Konrad Joachim Böhm, Igor Ivanov, Jahan B. Ghasemi, Elham Aghaee, and Klaus Müller

J. Med. Chem., **Just Accepted Manuscript** • DOI: 10.1021/acs.jmedchem.6b01591 • Publication Date (Web): 03 Jan 2017

ACS Publications

Journal of Medicinal Chemistry is published by the American Chemical Society. 1155 Sixteenth Street N.W., Washington, DC 20036

1

N-Heterocyclic (4-Phenylpiperazin-1-yl)methanones Derived from Phenoxazine and Phenothiazine as Highly Potent Inhibitors of Tubulin Polymerization

Helge Prinz*[,#], Ann-Kathrin Ridder[#], Kirsten Vogel[#], Konrad J. Böhm[f], Igor Ivanov[‡], Jahan B. Ghasemi[§], Elham Aghaee[§], Klaus Müller[#]

[#]*Institute of Pharmaceutical and Medicinal Chemistry, Westphalian Wilhelms-University, Corrensstraße 48, D-48149 Münster, Germany,* [f]*Leibniz Institute on Aging – Fritz Lipmann Institute (FLI), Beutenbergstrasse 11, D-07745 Jena, Germany,* [‡]*Oncolead GmbH & Co. KG, Zugspitzstraße 5, D-85757 Karlsfeld, Germany,* [§]*Drug Design in Silico Lab, Chemistry Faculty, School of Sciences, University of Tehran, Teheran, Iran*

[#] Institute of Pharmaceutical and Medicinal Chemistry, Westphalian Wilhelms-University

[f] Leibniz Institute on Aging – Fritz Lipmann Institute (FLI)

[‡] Oncolead GmbH & Co. KG

[§] Drug Design in Silico Lab, University of Tehran

Abstract

We report here a series of twenty-seven 10-(4-phenylpiperazin-1-yl)methanones derived from tricyclic heterocycles which were screened for effects on tumor cell growth, inhibition of tubulin polymerization, and induction of cell cycle arrest. Several analogs, among them the 10-(4-(3-methoxyphenyl)piperazine-1-carbonyl)-10*H*-phenoxazine-3-carbonitrile (**16o)**, showed excellent antiproliferative properties, with low nanomolar GI_{50} values (**16o**, mean GI_{50} of 3.3 nM) against a large number (93) of cancer cell lines. Fifteen compounds potently inhibited tubulin polymerization. Analysis of cell cycle by flow cytometry revealed that inhibition of tumor cell growth was related to an induction of G2/M phase cell cycle blockade. Western blotting and molecular docking studies suggested that these compounds bind efficiently to β-tubulin at the colchicine binding site. Our studies demonstrate the suitability of the phenoxazine and phenothiazine core and also of the phenylpiperazine moiety for the development of novel and potent tubulin polymerization inhibitors.

Introduction

Microtubules are key components of the cytoskeleton and play vital roles in essential eukaryotic cellular processes, such as organizing the spatial distribution of organelles throughout interphase, cell motility, vesicle transport and segregation of chromosomes during cell division.[1] Cancer cells grow and divide in an uncontrolled manner. Assembly of tubulin leads to the formation of the mitotic spindle apparatus, which is one of the most important targets in cancer chemotherapy.[2,3] The encouraging prospects of microtubule-targeted drugs for anticancer therapy stimulated intensive investigations aimed at the development of novel small-molecular tubulin binders by an integrative approach. This is not only based on the large-scale screening of compound libraries but also on the identification of active ingredients from natural materials, such as plant extracts, marine sources or traditional remedies.[4-6] Many cytotoxic agents exert their effects by inhibition of tubulin polymerization or by stabilizing microtubules.[5-9] As a result, cell division is inhibited by arresting cells specifically in the G2/M phase of the cell cycle, leading to cell death and the induction of apoptosis.

Tricyclic heterocycles are important scaffolds for a variety of different drugs.[10] The most common tricyclic ring is the phenothiazine (**1a**) as the core structure of the phenothiazin antipsychotics, with chlorpromazine (**2**) being the most prominent representative. Phenothiazines (**1a**, Chart 1) are related to a wide variety of pharmacological effects, such as psychotropic, anticancer,[11] antihelminthic and other properties.[12] We recently reported the discovery of N-benzoylated phenothiazine- and phenoxazine (**3a**) derivatives as tubulin polymerization inhibitors with potent *in vitro* antitumor activities.[13] Within the series, we identified **4** (Chart 1) as a highly active analogue. In continuation of this work, we here focus on the synthesis and biological testing for (4-phenylpiperazin-1-yl)methanones derived from phenothiazine, phenoxazine and structurally related analogs. The arylpiperazine scaffold has been classified as a privileged structure[14] for lead discovery and optimization and functions as an important and often recurring cyclic component of numerous drugs across a wide spectrum

of pharmacological properties.[15,16] Findings from recent literature prove the importance of the phenylpiperazine structural element for the development of tubulin polymerization inhibitors. About a decade ago, a series of ketopiperazides prepared from aryl- or heteroaryl carboxylic acids and diverse piperazines were described as potent, small-molecule tubulin polymerization inhibitors (**5**, Chart 2).[17,18] It is only recently that Ishii et al. revealed the phenylpiperazine-based α1-adrenoceptor (AR) antagonist naftopidil (**6**) as a tubulin-binding drug.[19] Also, chlorophenylpiperazine AK301 (**7**) has been identified as an inhibitor of tubulin polymerization and an effective sensitizer of cancer cells to apoptotic ligands.[20] Furthermore, (*E*)-3-(3,4-dihydroxyphenyl)acrylylpiperazine derivatives as exemplified by **8** have been described by Yin et al. as potent tubulin polymerization inhibitors.[21]

Inspired by the above literature findings and on basis of the encouraging data set obtained with our N-benzoylated tubulin polymerization inhibitors,[13] we considered the synthesis and evaluation of phenothiazine– and phenoxazine–derived (4-phenylpiperazin-1-yl)methanones particularly interesting. The most active compounds of this work exerted strong growth inhibitory potencies in the low submicromolar range across a wide range of tumor cell lines, closely related to potent inhibition of tubulin polymerization and concentration-dependent induction of cell cycle arrest. Notably, SAR results were distinct from our previously characterized N-benzoylated analogs. The most potent of the newly synthesized compounds had effects comparable or superior to those of known inhibitors, such as nocodazole, podophyllotoxin and colchicine.

Chemistry

The N-heterocyclic (4-phenylpiperazin-1-yl)methanones were prepared according to the method depicted in Scheme 1. Phenothiazines **1a** and **1b**, phenoxazines **3a-3d**, 1-phenylpiperazines, 5*H*-dibenzo[*b,f*]azepine **9**, 10,11-dihydro-5*H*-dibenz[*b,f*]azepine **10**, acridone **11**, diphenylamine **12**, 2-phenoxyaniline **13,** anilines, and benzylamine precursors

for **22a-22b** were purchased or synthesized according to literature methods. The starting 2-chloro-10*H*-phenoxazine **3b** and 2,8-dichloro-10*H*-phenoxazine **3c** were prepared in five steps starting via a 2-amino-2´-chlorodiaryl ether according to literature procedures.[22] The 10*H*-phenoxazine-3-carbonitrile **3d** was prepared as described by Eastmond et al.[23] In general, synthesis of various intermediate carbamoyl chlorides **14** was accomplished without isolating them by chlorocarbonylation of *N*-heterocycles or secondary amines with bis(trichloromethyl) carbonate[24] in 1,2-dichloroethane and pyridine, as illustrated in Scheme 1. Then, the desired (4-phenylpiperazin-1-yl)methanones **15a-15h, 16a-16p**, **17a-17b** and **18** were successfully obtained by carbamoylation of the appropriate 1-phenylpiperazines. In a similar fashion, *N*-phenyl-10*H*-phenoxazine-10-carboxamide **21** as well as *N*-benzyl-10*H*-phenoxazine-10-carboxamides **22a-22b** (Scheme 1) were prepared by reaction of phenoxazine-derived carbamoyl chlorides with diverse anilines or benzylamines, respectively. The synthesis of 1-(10*H*-phenoxazin-10-yl)-2-(4-phenylpiperazin-1-yl)ethan-1-ones **24a-24b** (Scheme 2) was accomplished via the 2-chloro-1-(10*H*-phenoxazin-10-yl)ethan-1-one **(23)**, which was obtained by initial chloroacylation of **3a** with chloroacetyl chloride under reflux in toluene,[25] and subsequent reaction with 1-(methoxyphenyl)piperazines. Despite a promising literature protocol,[24] several attempts to further modify the tricyclic heterocycle by carbamoylation of acridone **11** did not give any desired 10-(4-phenylpiperazine-1-carbonyl)acridin-9(10*H*)-one such as **26** (Scheme 3). Repeated attempts clearly revealed the formation of phenylpiperazinylacridines **27a-27f** instead. In this context, acylation of acridone to yield 10-benzoylacridin-9(10*H*)-one **25**, also failed (Scheme 3). Reaction of acridone **11** with benzoyl chloride gave the phenolic ester **28** instead of amide **25**.

Biological Results and Discussion

In Vitro Cell Growth Inhibition Assay

We preliminarily evaluated the cytotoxicity of the compounds towards K562 cells (human

chronic myelogenous leukemia, DSMZ ACC-10).[26] After 48 h of treatment, cell proliferation was quantified by counting the cells using a Neubauer hemocytometer. We routinely use this cell line as a suitable in vitro model, since treatment with anti-tubulin drugs characteristically alters the round-shaped cells and induces the formation of elongated angular forms within 1-2 hours.[27,28] Antiproliferative activities against K562 are expressed in Tables 1, 2 and 3, together with the data for the inhibition of tubulin polymerization (*see below*). Data for the positive controls are also included. Our nhibitory data cover a wide range of activities, with a high information content. Regarding the phenothiazine– and phenoxazine derivatives, ten compounds (**15b-15c**, **15g**, **16a**, **16c-16d**, **16j-16k, 16n** and **16o**) showed excellent growth inhibition in the nanomolar range (IC_{50} values ≤ 30 nM). This finding could be confirmed on the panel screening *(see* below). In contrast to its inactive (IC_{50} K562 > 30 μM) N-benzoylated analog,[13] phenothiazine-based (4-phenylpiperazin-1-yl)methanone **15a**, also being devoid of any ring substitutents – showed potent K562 cell growth inhibitory properties (IC_{50} 0.13 μM). Likewise, similar but more distinctive antiproliferative potencies were observed for phenoxazine-derived **16a** (IC_{50} 0.03 μM), being nearly equipotent with methoxy-substituted analogs **16c** and **16d**. In general, the introduction of a *para*-methoxy group in the terminal phenyl ring caused a marked loss in antiproliferative potency (e.g., **15b-15c**, IC_{50} 0.02 μM vs. **15d**, IC_{50} 3.70 μM; **16c-16d**, IC_{50} 0.02 μM vs. **16e**, IC_{50} 3.13 μM; **16o**, IC_{50} 0.007 μM vs. **16p**, IC_{50} 3.70 μM). On the other hand, methoxy groups located *ortho*- or *meta* strongly promoted potency. This result runs contrary to our findings among the N-benzoylated analogs,[13] where a *para*-methoxy-substitution turned out to be optimal. Consistent with the pattern in the phenothiazine series, phenoxazine analogues bearing *ortho*- or *meta*-methoxy substitutents in the phenylpiperazine scaffold **(16c**, IC_{50} 0.02 μM and **16d**, IC_{50} 0.02 μM), respectively) were most active, confirming that a *para*-methoxy substitution is less favorable in the terminal phenyl ring. Cell growth inhibitory activities of **16c-16d** proved identical to those of the corresponding phenothiazines **15b-15c**.

In the phenothiazine series, the introduction of additional substituents into the tricyclic nucleus did not contribute to improvement of antiproliferative potencies. Chloro-substituted phenothiazine analogue **15f** (IC_{50} K562 0.09 μM), for example, appeared nearly 5-fold less active than **15b** (IC_{50} 0.02 μM), whereas in case of the corresponding phenoxazine **16j** (IC_{50} K562 0.03 μM) potency was retained in comparison with **16c** (IC_{50} K562 0.02 μM). Moreover, the dichloro-substituted phenoxazines **16l (**IC_{50} K562 IC_{50} 0.13 μM) and **16m** (IC_{50} K562 IC_{50} 0.18 μM) were potent submicromolar inhibitors but were less active than the monochloro analogs, demonstrating that the 2,7-disubstitution doesn´t entail any additional advantage in terms of antiproliferative potencies. In good agreement with our previous observations,[13] outstanding antiproliferative potencies in the phenoxazine series could be attributed analogs bearing a a cyano functional group at the 3-position of the phenoxazine. Overall, the 10-(4-(3-methoxyphenyl)piperazine-1-carbonyl)-10*H*-phenoxazine-3-carbonitrile **(16o)** was the most active compound, which inhibited K562 cell growth with an IC_{50} of 7 nM. In this context, several aspects concerning the biological function of the nitrile group reviewed by Fleming et al.,[29] might be of interest.

In general, electron-withdrawing *para*-substituents in the terminal phenyl ring, such as trifluoromethyl (**16g**, IC_{50} K562 > 60 μM), nitro (**16h**, IC_{50} K562 > 70 μM), or cyano (**16i**) were considered weak to inactive and showed strongly reduced antiproliferative activities versus the most active compounds. Another interesting compound is **16f**. Given the fact, that chloro analog **16f** showed good activities and proved 5-fold more active than *para*-methoxy-substituted **16e** against K562 cells, the synthesis of *ortho*- or *meta*-chloro analogs – *meta*-chloro is also present in the structure of **7** (Chart 2) - should also be a very promising approach.

The comparison of the IC_{50} values obtained for phenylpiperazines **15d** or **16e** with those obtained for *N*-phenyl substituted compound **21** (Scheme 1, K562 IC_{50} > 80 μM) clearly demonstrated that the piperazine ring is a key structural element and contributes to potency.

As an interesting subsidiary aspect in terms of SAR, the result obtained with **21** demonstrates at the same time that the amide group shown in **4** (Chart 1), a representative and active N-benzoylated analog, can obviously not be successfully replaced by a urea structural element. The mere presence of a urea structural element, lacking the piperazine, obviously leads to weakly active or inactive compounds. This result is backed up by the replacement of the phenylpiperazine by a benzylamine (**22a,** IC_{50} 6 μM; **22b**, 19 μM, Table 3, Chart 3), which also resulted in low potencies in comparison with **16c** and **16d** (Table 2). Incorporating a bridging methylene as seen with **24a-24b** caused a dramatic loss of antiproliferative potency (**24a**, IC_{50} 9 μM, and **24b**, IC_{50} 5 μM, respectively, vs. **16c**, IC_{50} 0.02 μM). This result confirms, once again, that the intact (4-phenylpiperazin-1-yl)methanone is particularly important for antiproliferative activity.

When testing alternative scaffolds, ring-opened diphenylamine analog **19** proved considerably less effective compared to the most active analogs (**19**, IC_{50} K562 18 μM vs. **15c**, IC_{50} K562 0.02 μM or **16d**, IC_{50} K562 0.02 μM), indicating that rigidifying the diphenylamine is important for target binding. The same observations were made on ring-opened 2-phenoxyaniline-based analogues **20a-20c** (Scheme 1, Table 3), which were not active. Interestingly, decreasing the ring size to obtain carbazoles (6-5-6 fused) induced strong potencies (< 100 nM for the most active analogs, *manuscript in preparation*). Also, the ring-expanded (6-7-6 fused) 5*H*-dibenzo[*b*,*f*]azepines **17a-17b** (**17a**, IC_{50} K562 0.45 μM and **17b**, IC_{50} K562 0.94 μM, respectively) as well as the dihydro analog **18** (IC_{50} K562 0.84 μM) were submicromolar, potent inhibitors of K562 cell growth, but proved clearly less active than the most active analogs. To complement this, 9-(4-(phenyl)piperazin-1-yl)acridines **27a-27f,** lacking the carbonyl compared with **5** (Chart 2), were inactive or only weakly active (K562 IC_{50}: **27a**, 4.5 μM; **27b** 8.8 μM, **27c-27f** > 10 μM).

Cell Panel Screen

Cell-based cancer screening panels in combination with data analysis and interpretation can be of great value for assigning a molecular target to test compound action and allows hit prioritization for additional studies. Therefore, we explored the potencies of twelve selected compounds (**15a-15c**, **15g-15h**; **16a**, **16c**, **16e**, **16j-16k**, **16n-16o**) against a broad range (93, + resting, non-proliferating PBMCs) of tumor cell lines.[30] Visualization of results by mean graphs provides a compact way to mirror profiles of relative sensitivity and resistance of cellular parameters in response to treatment of mutiple cell lines with potential anticancer drugs.[31] Our screening included a large panel of tumor cell lines (93), covering multiple tumor types. In addition, resting, non-proliferating peripheral blood mononuclear cells[32] (PBMC) were included in the studies. For quantification of cell proliferation, cells were stained with fluorescent dye sulforhodamine B (SRB).

Our results from the panel screening proved the outstanding overall antiproliferative potencies (GI_{50}, the molar concentration causing 50% cell growth inhibition in relation to the initial cell seeding number) of cyano-substituted analogs **16n** and **16o**, evidenced by extremely low nanomolar mean GI_{50} values over all tumour cell lines (93) tested (**16n**, mean GI_{50} of 4.1 nM and **16o,** mean GI_{50} of 3.3 nM, respectively). Compounds **15a-15c** and **15g** as well as **16a**, **16c**, and **16j-16k** showed also strong potencies with mean GI_{50} data in the range of 14-35 nM (see SI for details). Among the analogs tested the panel screen, as expected, **15h** and **16e** were the least active, with GI_{50} data of 1.57 and 1.97 μM, respectively. Noteworthy, when comparing the GI_{50} values for **16n** and **16o** with previously described N-benzoylated **4**[13] (Chart 1), some divergences became quite striking. On the one hand, GI_{50} data of **16n**, **16o** and **4** (83 cell line screening, same method) against the most sensitive cell lines were quite similar (≤ 10 nM), whereas GI_{50} data observed for the eight most resistant cell lines strongly differed, covering a wide range in the case of **4** (60 nM up to 8.5 μM)[13] but retaining high nanomolar potencies in a narrow span for **16n** (GI_{50} 7.0-15.6 nM) and **16o** (GI_{50} 5.9-7.9 nM),

respectively. This finding clearly indicates more distinct antiproliferative properties of the (4-phenylpiperazin-1-yl)methanones in overall cell lines compared to the N-benzoylated analogs. We used a mean graph display format for visualization of the 8 most sensitive and most resistant cell lines, or, alternatively, a box-plot graph (Table 4, Fig. 1 A, B). Briefly, horizontal bars extending to the right from the zero value refer to less sensitive cell lines, bars extending to the left indicate more resistant cell lines. Each bar, therefore, represents the relative activity of the compound in the given cell lines deviating from the mean in all cell lines (GI_{50}). No activity could be detected in quiescent peripheral blood mononuclear cells (PBMC), suggesting that antiproliferative activities are related to actively cycling cells.

In Vitro-Tubulin Polymerization Assays

Next, we explored the effect of the compounds on tubulin polymerization. Colchicine, podophyllotoxin, nocodazole, and vinblastine were used as reference compounds (Table 1). Self-assembly of αβ-tubulin is usually followed by an increase in turbidity at 340-360 nm over a 45 min period at 37 °C.[33] This is based on the fact, that light scattering by microtubules is proportional to the amount of microtubule polymer. Usually, typical sigmoidal tubulin polymerization curves are obtained, with a plateau reached with the steady state equilibrium level. Typically, in response to a microtubule destabilizer, the level of steady state turbidity decreases in a dose–dependent manner, as exemplified for **16o** (Figure 2, A).

Figure 2 should be inserted here

Thirteen compounds **(15a-15c**, **15f-15g**, **16c-16d**, **16f**, **16j-16k**, **16m-16o**) proved to be potent tubulin assembly inhibitors ($IC_{50} \leq 1$ μM), with potencies comparable or superior to the reference anti-tubulin drugs. These strong potencies, in particular those of **16n** and **16o**, were in excellent correlation with the data from the cellular proliferation assay. The most active

inhibitors of tumor cell growth were also the most effective inhibitors of tubulin polymerization. The 2-methoxy- as well as the 3-methoxy-substituted substituted compounds showed the greatest potency. Additionally, in good agreement with the cellular assays, strong tubulin polymerization inhibiting properties can also be found with **15a** as well as **16a**, both being unsubstituted phenylpiperazine scaffold. Moreover, compound **16l** was slightly more potent than colchicine, whereas analogous **17a-17b** were moderate inhibitors of tubulin polymerization. In general, compounds having IC_{50} values in the range of ≥ 10 μM showed no appreciable activity as an inhibitor of tubulin polymerization, which applied to phenothiazine-derived **15h** and phenoxazines **16g-16i** (Table 1, 2) and several structurally related analogues (Table 3). An overview of the resulting SAR from the cell-based assay and the tubulin assembly assay is depicted in Fig. 5.

EBI Competition Assay

Microtubule-destabilizing as well as destabilizing drugs are known to interact with tubulin through different binding sites.[34] To explore whether compounds **15b** and **16o** directly interact with tubulin at the colchicine-binding site, we performed a competition assay with N,N′-ethylene-bis(iodoacetamide) (EBI) in K562 cells.[35-37] As an alkylating agent, EBI has the property to cross-link the Cys239 and the Cys354 residues of β-tubulin involved in the colchicine-binding site. The EBI-assay is based on the fact, that – in the absence of a potential colchicine binding agent - the EBI/β-tubulin adduct can be detected as an immunoreactive β-tubulin band that can be seen below the β-tubulin band in the Western blot. So, if EBI is added to cells previously treated with a colchicine-site binder, the binding site is already occupied and the EBI adduct cannot be observed. Thus, compounds that bind to the colchicine-binding site in β-tubulin prevent the formation of the EBI:β-tubulin adduct. Colchicine (5 μM) as well as **15b** (20 μM and 40 μM, respectively) and **16o** (14 μM and 7 μM, respectively) prevented the binding of EBI to β-tubulin in living K562 cells (Fig. 3),

resulting in the absence of the adduct band. Therefore, we consider it very likely that the novel compounds exert their biological activities by binding to the colchicine-binding site of β-tubulin.

Figure 3 should be inserted here

Effect on Cell-Cycle Progression

Tubulin polymerization inhibitors suppress microtubule formation and induce cell cycle arrest during interphase at G2/M, a hallmark of tubulin polymerization inhibitors. As a result, chromosome separation is seriously impaired.[38,39] Dose-dependent effects on the cell cycle were studied in K562 cells (**15c**, **16c-16d**, **16o**) and percentage distribution of cells on cell-cycle phases was measured (see SI). It became evident that phenoxazine–derived **16o** accumulated cells at G2/M at concentrations down to 30 nM (Fig. 4), comparable to colchicine, which served as positive G2/M arrest control. A normal cell cycle distribution was observed in the vehicle-treated control cells.

Figure 4 should be inserted here

Our findings indicate that the compounds in this paper, as represented by **16n**, can be classified as potent antimitotic drugs that arrest proliferating cells at G2/M.

Figure 5 should be inserted here

Binding model of compounds 16n with tubulin

In recent years, 3D-quantitative structure-activity relationship (3D-QSAR) and docking studies have widely been used to predict inhibitory activities of new tubulin polymerization

inhibitors.[40-42] To gain insight on the possible binding mode the novel 10-(4-phenylpiperazin-1-yl)methanones and to create predictive 3D-QSAR models, CoMFA and CoMSIA analyses were performed. Due to its high tubulin binding activity, compound **16n** was used as a template.

The comparative molecular field analysis (CoMFA) uses data from known active molecules and is an important 3D-QSAR method which focuses on non-bonding interactions between the protein and the ligand. It provides a common way to display electrostatic (Coulombic) and steric (Lennard-Jones) fields of the regions important for biological activity.[43] An alternative computational approach is the comparative molecular similarity indices analysis (CoMSIA), which employs a distance-based Gaussian-type function to evaluate five molecular fields of different physico-chemical properties (i.e. steric, electrostatic, hydrophobic, and hydrogen bonding donor and acceptor).[44,45]

Docking results

Molecular docking was used as a computational tool to gain insight into the binding mode of the novel 10-(4-phenylpiperazin-1-yl)methanones. As a parameter of docking accuracy, we calculated a high-level root-mean-square distance (RMSD) value of 0.774 Å between bound ligand and re-docked colchicine. This value documents the reliability of GOLD for the reproduction and identification of the correct binding mode of a lead compound. Based on our docking studies, there is a hydrogen bond between the methanone C=O group and Val181 from the α chain. Furthermore, when focusing on the binding mode of the best docked pose of compound **16n**, two cation-π interactions between the phenyl rings and Lys352 and Lys254 of tubulin β chain were identified (Fig. 6).

Fig. 6 should be inserted here.

CoMFA and CoMSIA results

The results from the 3D-QSAR studies are summarized in Tables 1-3 (see SI). Partial least squares (PLS) regression analysis of the compounds in training set showed a CoMFA-region focusing (CoMFA-RF) QSAR model (grid spacing = 1) with an excellent *q2* value of 0.829 (3 components), indicating significant predictive properties. The non cross-validated PLS analysis revealed a high squared correlation coefficient r^2 value of 0.957 and a high predictive correlation coefficient (r^2_{pred}) of 0.759. Fig. 7. presents the relationship between the experimental and predicted pIC_{50} (Table 1, SI).

Fig. 7 should be inserted here.

The CoMFA-RF steric and electrostatic fields from the final best non cross-validated analysis were plotted as 3D colored contour maps (Fig. 8). A large region of green colour near R^4 and R^5 (general structure Table 2) in the 3D coloured contour map suggested that the introduction of bulky substituents such as methoxy would lead to potent analogs. This is confirmed by different activities of compounds **16c** ($R^4 = OCH_3$, $pIC_{50} = 6.194$) and **16d** ($R^5 = OCH_3$, $pIC_{50} = 6.161$) compared with **16a** ($R^4 = R^5 = H$, $pIC_{50} = 5.860$).

Fig. 8 should be inserted here.

A red contour placed near R^4 and R^5 substituents indicates that electronegative groups such as methoxy group contribute to an increase in antiproliferative potencies. Also, a small red contour near the R^2 substituent demonstrates that electronegative groups such as CN are favorable and increase the potency. This is the reason why cyano-substituted compounds **16n** and **16o** are among the most active analogs of all compounds tested. Moreover, a blue region near R6 indicates that electropositive substituents such as H would increase the potency.

CoMSIA as an analysis tool was performed using a lattice box with a grid spacing of 2 Å and the combination of fields was systematically varied to obtain the best results. CoMSIA PLS analysis yielded a good q^2 value of 0.729, a high r^2 value of 0.958 and gave a high predictive correlation coefficient (r^2_{pred}) of 0.813 with 3 PLS components by using the combination of five fields (steric, electrostatic, hydrophobic, hydrogen bond donor and acceptor). When comparing contour maps obtained from both the CoMSIA and the CoMFA approach, some similarities became obvious (Fig. 9). The visual display of the CoMSIA steric contour maps shows, as indicated by the yellow colour, that less steric groups near substituents R^6 and R^3 would increase antiproliferative potencies. On the other hand, the large green contour reveals that more bulky substituents such as methoxy near R^4 and R^5 would promote the formation more potent analogs. With reference to the hydrophobic contour map of CoMSIA, the white contour near the R^4 and R^5 substituents suggests that more hydrophilic groups at this position would increase the activity. A yellow contour near R^6 emphasises the need for hydrophobic groups in this area to promote tubulin-inhibitory properties.

Fig. 9 should be inserted here.

The magenta contours near the R^2 and C=O substituents point towards regions where hydrogen bond acceptor groups are favored, whereas red contours mark regions where hydrogen bond acceptor groups are less favorable for binding. Obviously, there is a hydrogen bond donor (Val181) which effectively complements the C=O in the receptor. Also, the electrostatic red contour at the R^2 region and the magenta contour near the R^2 substituent complement each other.

Conclusion

Synthesis and focused SAR studies for phenylpiperazinylmethanones derived from a

phenothiazine and phenoxazine structural scaffold as novel anti-tubulin agents were performed. The novel compounds showed excellent potencies as inhibitors of tumour cell growth and tubulin polymerization. The most promising analogs, represented by 10-(4-(3-methoxyphenyl)piperazine-1-carbonyl)-10*H*-phenoxazine-3-carbonitrile (**16o**), inhibited tubulin polymerization in the range of the positive controls and proved highly active in comprehensive cell-based cancer screening panels, as evidenced by exceptionally low nanomolar mean GI_{50} values over all tumour cell lines (93) tested (**16n**, mean GI_{50} of 4.1 nM and **16o,** mean GI_{50} of 3.3 nM, respectively). The most active analogs showed two essential moieties. One is the tricyclic (6-6-6) phenothiazine or phenoxazine scaffold. The second is the intact phenylpiperazinylmethanone structure. Taken together, our findings highlight not only the phenoxazine and phenothiazine but also the phenylpiperazine moiety as important structural elements for inhibition of tubulin polymerization.[4,5] The presence of *ortho*- or *meta*-methoxy groups in the phenylpiperazine or – somewhat surprising – an unsubstituted phenyl turned out to be crucial for growth inhibitory potencies and impairment of tubulin assembly into microtubules. We conclude that the growth inhibitory properties are most likely mediated through an impairment of tubulin polymerization, as documented by the EBI assay and the fact that the most potent inhibitors of cancer cell growth turned out to be the most efficacous tubulin assembly inhibitors. Closely related to this, key representatives such as **16o** blocked the cell cycle at the G2/M phase at concentrations down to 30 nM. CoMFA and CoMSIA approaches provided useful insights into the binding of the analogs in tubulin. We could once again confirm that a nitrile functional group placed at the 3-position of the phenoxazine scaffold significantly contributes to antiproliferative properties.

In summary, we envision that N-heterocyclic (4-phenylpiperazin-1-yl)methanones hold great potential for further structural modifications and we believe that our studies provide some valuable information for the design of effective anti-cancer drugs. Additional studies on the synthesis and biological activities of further analogues are in progress and the results are

being published in due course.

Experimental Section

Melting points were determined with a Kofler melting point apparatus and are uncorrected. ^{1}H NMR (600 MHz, 400 MHz) and ^{13}C NMR (151 MHz, 100 MHz) were obtained on an Agilent 600-MR, Agilent 400-MR, and Mercury Plus AS 400 NMR spectrometer (Varian); δ in ppm related to tetramethylsilane. Fourier-transform IR spectra were recorded on a Jasco FT/IR-4100 (attenuated total reflection, ATR) spectrometer by applying ATR correction. Mass spectra were obtained on Finnigan MAT GCQ and LCQ apparatuses applying electron beam ionization (EI) and electrospray ionization (ESI). Atmospheric pressure chemical ionization (APCI) method was performed with a micrOTOF-QII apparatus (Bruker Daltonics´, Bremen, Germany) and APCI II-interface or ESI-interface (Bruker Daltonics´, Bremen, Germany). The purity of all target compounds was determined by reversed phase HPLC at 254 nm. Compound purity, as determined by analytical reversed-phase HPLC for all target compounds, is ≥ 95%. The HPLC system applied a C18 phase (Nucleosil, 3 μm, 4.0 × 125 mm, CS-Chromatographie Service GmbH, Langerwehe, Germany) eluting the compounds with an acetonitrile/H_2O gradient at a flow rate of 0.40 mL/min. All organic solvents were appropriately dried or purified prior to use. Purification by chromatography refers to column chromatography on silica gel (Macherey-Nagel, 70-230 mesh). In most cases, the concentrated pure fractions obtained by chromatography using the indicated eluants were treated with a small amount of *n*-hexane to induce precipitation. All new compounds displayed ^{1}H NMR, ^{13}C NMR and MS spectra consistent with the assigned structure. Yields have not been optimized. Analytical TLC was done on Merck silica 60 F_{254} alumina coated plates (E. Merck, Darmstadt).

2-Chloro-10*H*-phenoxazine (3b).

The title compound was prepared according to the literature protocol.[46]

2,8-Dichloro-10*H*-phenoxazine (3c).

The title compound was prepared according to the literature protocol.[13]

10*H*-phenoxazine-3-carbonitrile (3d).[23]

The title compound was prepared according to the literature protocol.

(10*H*-Phenothiazin-10-yl)(4-phenylpiperazin-1-yl)methanone (15a). The title compound was prepared from **1a** (2 mmol, 0.40 g) and 1-phenylpiperazine (0.32 g, 2 mmol) in 1,2-dichloroethane (20 mL) and pyridine (1 mL) in a similar manner as described for **15g**. Purification by chromatography (ethyl acetate / petroleum ether, 3:7) afforded **15a** as a white powder (0.27 g, 35%). mp 141-142 °C; FTIR: 1647 cm^{-1} (C=O); ^1H NMR (400 MHz, $CDCl_3$) δ 7.69 (dd, *J* = 8.1, 1.3 Hz, 2H), 7.32 (dd, *J* = 7.7, 1.5 Hz, 2H), 7.27 – 7.20 (m, 4H), 7.11 (td, *J* = 7.5, 1.3 Hz, 2H), 6.87 (q, *J* = 6.4, 4.9 Hz, 3H), 3.53 (t, *J* = 5.1 Hz, 4H), 3.11 – 2.98 (m, 4H); ^{13}C NMR (101 MHz, $CDCl_3$) 157.19, 141.34, 129.20, 128.94, 127.69, 127.56, 127.30, 125.23, 122.25, 120.40, 116.49, 48.94, 45.64; MS (APCI) calcd for $C_{23}H_{21}N_3OS$ $[M+H]^+$ 388.1484; found 388.1467; purity (HPLC): 99.48 %.

(4-(2-Methoxyphenyl)piperazin-1-yl)(10*H*-phenothiazin-10-yl)methanone (15b). The title compound was prepared from **1a** (2 mmol, 0.40 g) and 1-(2-methoxyphenyl)piperazine (0.38 g, 2 mmol) in 1,2-dichloroethane (20 mL) and pyridine (1 mL) in a similar manner as described for **15g**. Purification by chromatography (ethyl acetate / petroleum ether, 3:7) afforded **15b** as a white powder (0.23 g, 28%). mp 163 °C; FTIR: 1659 cm^{-1} (C=O); ^1H NMR (400 MHz, $CDCl_3$) δ 7.68 (dd, *J* = 8.1, 0.9 Hz, 2H), 7.30 (dd, *J* = 7.7, 1.3 Hz, 2H), 7.27 – 7.21 (m, 2H), 7.10 (td, *J* = 7.6, 1.2 Hz, 2H), 7.03-6.98 (m, 1H), 6.92 – 6.82 (m, 3H), 3.83 (s, 3H), 3.57 (s, br, 4H), 2.93 (s, br, 4H); ^{13}C NMR (101 MHz, $CDCl_3$) 157.06, 152.14, 141.43, 128.60, 127.64, 127.56, 125.10, 123.42, 121.96, 121.01, 118.32, 111.25, 77.32, 77.20, 77.00, 76.68, 55.38, 50.25, 45.87; MS (EI, 70 eV) *m/z* (%) 417 (26), 219 (100); purity (HPLC): 98 %.

(4-(3-Methoxyphenyl)piperazin-1-yl)(10*H*-phenothiazin-10-yl)methanone (15c). The title compound was prepared from **1a** (2 mmol, 0.40 g) and 1-(3-methoxyphenyl)piperazine (0.38 g, 2 mmol) in 1,2-dichloroethane (20 mL) and pyridine (1 mL) in a similar manner as described for **15g**. Purification by chromatography (ethyl acetate / petroleum ether, 3:7) afforded **15c** as a white powder (0.35 g, 42%). mp 105 °C; FTIR: 1663 cm^{-1} (C=O); ^{1}H NMR (600 MHz, $CDCl_3$) δ 7.68 (dd, *J* = 8.2, 1.2 Hz, 2H), 7.32 (dd, *J* = 7.7, 1.5 Hz, 2H), 7.25 – 7.21 (m, 2H), 7.17 – 7.13 (m, 1H), 7.11 (td, *J* = 7.5, 1.3 Hz, 2H), 6.50 – 6.35 (m, 3H), 3.76 (s, 3H), 3.52 (s, br, 4H), 3.04 (s, 4H); ^{13}C NMR (151 MHz, $CDCl_3$) 233.89, 160.58, 160.56, 157.22, 152.15, 141.33, 129.90, 129.00, 127.71, 127.58, 127.49, 125.27, 122.31, 109.15, 105.06, 102.90, 55.21, 48.81, 45.59; MS (EI, 70 eV) *m/z* (%) 417 (28), 219 (100); purity (HPLC): 99.75 %.

(4-(4-Methoxyphenyl)piperazin-1-yl)(10*H*-phenothiazin-10-yl)methanone (15d). The title compound was prepared from **1a** (2 mmol, 0.40 g) and 1-(4-methoxyphenyl)piperazine (0.38 g, 2 mmol) in 1,2-dichloroethane (20 mL) and pyridine (1 mL) in a similar manner as described for **15g**. Purification by chromatography (ethyl acetate / petroleum ether, 3:7) afforded **15d** as a white powder (0.32 g, 38%). mp 116 °C; FTIR: 1670 cm^{-1} (C=O); ^{1}H NMR (600 MHz, $CDCl_3$) δ 7.68 (dd, *J* = 8.1, 1.2 Hz, 2H), 7.31 (dd, *J* = 7.7, 1.5 Hz, 2H), 7.24 (d, *J* = 1.3 Hz, 2H), 7.11 (dd, *J* = 7.5, 1.3 Hz, 2H), 6.81 (s, 4H), 3.75 (s, 3H), 3.52 (s, br, 4H), 2.91 (s, br, 4H); ^{13}C NMR (151 MHz, $CDCl_3$) δ 157.13, 141.36, 128.81, 127.66, 127.54, 125.17, 122.14, 118.68, 114.47, 60.37, 55.52, 50.40, 45.81; MS (EI, 70 eV) *m/z* (%); purity (HPLC): 100 %.

4-(4-(10*H*-Phenothiazine-10-carbonyl)piperazin-1-yl)benzonitrile (15e). The title compound was prepared from **1a** (2 mmol, 0.40 g) and 1-(4-cyanophenyl)piperazine (0.37 g, 2 mmol) in 1,2-dichloroethane (20 mL) and pyridine (1 mL) in a similar manner as described for **15g**. Purification by chromatography (ethyl acetate / petroleum ether, 3:7) afforded **15e** as a white powder (0.34 g, 41%). mp 217 °C; FTIR: 2222 (CN), 1647 cm^{-1} (C=O); ^{1}H NMR (400

MHz, $CDCl_3$) δ 7.70 (dd, *J* = 8.1, 1.3 Hz, 2H), 7.50 – 7.43 (m, 2H), 7.34 (dd, *J* = 7.7, 1.5 Hz, 2H), 7.28 – 7.22 (m, 2H), 7.14 (dd, *J* = 7.6, 1.3 Hz, 2H), 6.81 – 6.74 (m, 2H), 3.53 – 3.45 (m, 4H), 3.24 – 3.16 (m, 4H); ^{13}C NMR (101 MHz, $CDCl_3$) δ 157.36, 152.66, 141.13, 133.53, 129.50, 127.79, 127.60, 125.48, 122.67, 119.69, 114.39, 101.14, 46.69, 45.15; MS (APCI) calcd for $C_{24}H_{21}N_4OS$ $[M+H]^+$ 413.1436; found 413.1471; purity (HPLC): 99.25 %.

(2-Chloro-10*H*-phenothiazin-10-yl)(4-(2-methoxyphenyl)piperazin-1-yl)methanone (15f). The title compound was prepared from **1b** (2 mmol, 0.47 g) and 1-(2-methoxyphenyl)piperazine (0.38 g, 2 mmol) in 1,2-dichloroethane (20 mL) and pyridine (1 mL) in a similar manner as described for **15g**. Purification by chromatography (ethyl acetate / petroleum ether, 3:7) afforded **15f** as a white powder (0.33 g, 37%). mp 151 °C; FTIR: 1651 cm^{-1} (C=O); ^{1}H NMR (400 MHz, $CDCl_3$) δ 7.88 (d, *J* = 2.1 Hz, 1H), 7.47 (dd, *J* = 8.1, 1.2 Hz, 1H), 7.29 (dd, *J* = 7.7, 1.5 Hz, 1H), 7.27 – 7.21 (m, 1H), 7.19 (d, *J* = 8.3 Hz, 1H), 7.14 – 7.05 (m, 2H), 7.05 – 6.98 (m, 1H), 6.93 – 6.81 (m, 3H), 3.83 (s, 3H), 3.60 (s, br, 4H), 2.94 (s, 4H); ^{13}C NMR (101 MHz, $CDCl_3$) 156.46, 152.16, 142.31, 141.17, 133.48, 128.04, 127.90, 127.82, 127.77, 126.44, 125.40, 124.99, 123.54, 121.85, 121.54, 121.03, 118.39, 111.26, 77.32, 77.20, 77.00, 76.68, 55.40, 50.25, 45.82. MS (EI, 70 eV) *m/z* (%) 451 (10), 219 (100); purity (HPLC): 99.41 %.

(2-Chloro-10*H*-phenothiazin-10-yl)(4-(3-methoxyphenyl)piperazin-1-yl)methanone (15g). In a typical procedure, a stirred mixture of 2-chlorophenothiazine **1b** (0.47 g, 2 mmol), bis(trichloromethyl) carbonate (0.356 g, 1.2 mmol), pyridine (1 mL) and 1,2-dichlororethane (20 mL) was heated under reflux (N_2 atmosphere, oil bath, 75 °C). After 3 h, formation of the intermediate carbamoyl chloride was completed (TLC control, dichloromethane / n-hexane, 1/1). Then, 1-(3-methoxyphenyl)piperazine (0.38 g, 2 mmol) was added in one portion. Stirring was continued after formation of the product appeared to be complete (2-3 h, TLC control, ethyl acetate / petroleum ether 40-60 °C, 3:7). The mixture was poured into H_2O (200 mL)/6M HCl (10 mL) and extracted with CH_2Cl_2 (3 × 30 mL). The combined organic layers

were washed with water and dried over Na_2SO_4. Then, the drying agent was removed by filtration and the solvent was evaporated in vacuum. The residue was then purified by silica gel chromatography (ethyl acetate/petroleum ether 40-60 °C, 3/7) to afford **15g** as a pale-yellow solid (0.40 g, 44 %). mp 118-119 °C; FTIR: 1663 cm^{-1} (C=O); ^{1}H NMR (600 MHz, $CDCl_3$) δ 7.90 (d, *J* = 2.1 Hz, 1H), 7.45 (dd, *J* = 8.2, 1.2 Hz, 1H), 7.31 (dd, *J* = 7.7, 1.5 Hz, 1H), 7.25 – 7.21 (m, 1H), 7.20 (d, *J* = 8.3 Hz, 1H), 7.18 – 7.07 (m, 3H), 6.51 – 6.38 (m, 3H), 3.77 (s, 3H), 3.57 – 3.50 (m, 4H), 3.06 (t, *J* = 5.2 Hz, 4H); ^{13}C NMR (151 MHz, $CDCl_3$) 160.60, 156.62, 142.16, 141.10, 133.50, 129.95, 128.35, 128.10, 128.09, 127.86, 126.82, 125.59, 125.17, 122.21, 121.87, 109.28, 105.24, 103.07, 60.40, 55.22, 48.96, 45.53, 14.21. MS (EI, 70 eV) *m/z* (%) 451 (29), 219 (100); purity (HPLC): 98.61 %.

(2-Chloro-10*H*-phenothiazin-10-yl)(4-(4-methoxyphenyl)piperazin-1-yl)methanone (15h). The title compound was prepared from **1b** (2 mmol, 0.47 g) and 1-(4-methoxyphenyl)piperazine (0.38 g, 2 mmol) in 1,2-dichloroethane (20 mL) and pyridine (1 mL) in a similar manner as described for **15g**. Purification by chromatography (ethyl acetate / petroleum ether, 3:7) afforded **15h** as a beige powder (0.23 g, 22%). mp 108-109 °C; FTIR: 1659 cm^{-1} (C=O); ^{1}H NMR (600 MHz, $CDCl_3$) δ 7.89 (d, *J* = 2.2 Hz, 1H), 7.47 – 7.43 (m, 1H), 7.30 (dd, *J* = 7.7, 1.5 Hz, 1H), 7.25 – 7.21 (m, 1H), 7.25 – 7.22 (m, 1H), 7.19 (d, *J* = 8.3 Hz, 1H), 7.14 – 7.05 (m, 2H), 6.85 – 6.79 (m, 3H), 3.75 (s, 3H), 3.59 – 3.50 (m, 4H), 2.95 – 2.90 (m, 4H); ^{13}C NMR (151 MHz, $CDCl_3$) δ 156.55, 154.35, 145.14, 142.24, 141.14, 133.49, 128.67, 128.42, 128.14, 128.08, 127.83, 127.77, 127.63, 127.26, 126.81, 126.64, 126.56, 125.50, 125.09, 122.11, 122.04, 121.72, 118.83, 114.50, 114.16, 113.01, 55.54, 51.28, 50.50, 45.81, 31.60, 22.66, 14.13; MS (EI, 70 eV) *m/z* (%) 451 (24), 219 (100); purity (HPLC): 87.48 %.

(10*H*-Phenoxazin-10-yl)(4-phenylpiperazin-1-yl)methanone (16a). The title compound was prepared from **3a** (2 mmol, 0.36 g) and 1-phenylpiperazine (0.32 g, 2 mmol) in 1,2-dichloroethane (20 mL) and pyridine (1 mL) in a similar manner as described for **15g**.

Purification by chromatography (ethyl acetate / petroleum ether 3:7) afforded **16a** as a white powder (0.36 g, 49%). mp 101-102 °C; FTIR: 1666 cm^{-1} (C=O); ^{1}H NMR (600 MHz, $CDCl_3$) δ 7.31 – 7.24 (m, 2H), 7.05 – 6.98 (m, 2H), 6.94 – 6.84 (m, 9H), 3.75 (t, *J* = 5.1 Hz, 4H), 3.22 – 3.14 (m, 4H); ^{13}C NMR (151 MHz, $CDCl_3$) δ 218.62, 154.27, 150.65, 145.71, 130.34, 129.30, 123.92, 123.91, 123.80, 120.77, 116.75, 116.50, 116.49, 116.14, 49.53, 45.21; MS (EI, 70 eV) *m/z* (%) 371 (20), 189 (100); purity (HPLC): 99.71 %.

(10*H*-Phenoxazin-10-yl)(4-(methylphenyl)piperazin-1-yl)methanone (16b). The title compound was prepared from **3a** (2 mmol, 0.36 g) and 1-(4-methylphenyl)piperazine (0.35 g, 2 mmol) in 1,2-dichloroethane (20 mL) and pyridine (1 mL) in a similar manner as described for **15g**. Purification by chromatography (ethyl acetate / petroleum ether, 3:7) afforded **16b** as a white powder (0.41 g, 54 %). mp 125-126 °C; FTIR: 1686 cm^{-1} (C=O); ^{1}H NMR (600 MHz, $CDCl_3$) δ 7.08 (d, *J* = 8.2 Hz, 2H), 7.02 – 6.97 (m, 2H), 6.92 – 6.85 (m, 6H), 6.84 – 6.79 (m, 2H), 3.74 (t, *J* = 5.1 Hz, 4H), 3.12 (t, *J* = 5.1 Hz, 4H), 2.27 (s, 3H); ^{13}C NMR (151 MHz, $CDCl_3$) δ 218.64, 154.23, 148.58, 145.64, 130.34, 129.81, 123.91, 123.75, 123.64, 117.07, 116.48, 116.45, 116.06, 115.87, 51.38, 50.05, 45.60, 45.26, 31.60, 22.67, 20.46, 14.14; MS (EI, 70 eV) *m/z* (%) 385 (21), 204 (15), 203 (100), 182 (16); purity (HPLC): 99.72 %.

(4-(2-Methoxyphenyl)piperazin-1-yl)(10*H*-phenoxazin-10-yl)methanone (16c). The title compound was prepared from **3a** (2 mmol, 0.36 g) and 1-(2-methoxylphenyl)piperazine (0.38 g, 2 mmol) in 1,2-dichloroethane (20 mL) and pyridine (1 mL) in a similar manner as described for **15g**. Purification by chromatography (ethyl acetate / petroleum ether, 3:7) afforded **16c** as a white powder (0.37 g, 46 %). mp 123 °C; FTIR: 1663 cm^{-1} (C=O); ^{1}H NMR (600 MHz, $CDCl_3$) δ 7.06 – 7.01 (m, 1H), 7.00 – 6.96 (m, 2H), 6.94 – 6.84 (m, 9H), 3.86 (s, 3H), 3.82 – 3.74 (m, 4H), 3.09 – 3.01 (m, 4H)); ^{13}C NMR (151 MHz, $CDCl_3$) δ 233.91, 154.16, 152.19, 152.18, 145.48, 140.42, 130.34, 123.90, 123.68, 123.60, 121.05, 118.42, 116.42, 115.87, 111.32, 55.43, 50.63, 45.49; MS (EI, 70 eV) *m/z* (%) 401 (24), 219 (100), 191 (14), 182 (17); purity (HPLC): 99.63 %.

(4-(3-Methoxyphenyl)piperazin-1-yl)(10*H*-phenoxazin-10-yl)methanone (16d). The title compound was prepared from **3a** (2 mmol, 0.36 g) and 1-(3-methoxylphenyl)piperazine (0.38 g, 2 mmol) in 1,2-dichloroethane (20 mL) and pyridine (1 mL) in a similar manner as described for **15g**. Purification by chromatography (ethyl acetate / petroleum ether, 3:7) afforded **16d** as a pale yellow powder (0.54 g, 67 %). mp 122 °C; FTIR: 1661 cm^{-1} (C=O); ^{1}H NMR (600 MHz, $CDCl_3$) δ 7.18 (t, *J* = 8.1 Hz, 1H), 7.04 – 6.98 (m, 2H), 6.93 – 6.84 (m, 6H), 6.47 (dd, *J* = 7.9, 2.2 Hz, 3H), 3.78 (s, 4H), 3.73 (t, *J* = 10.4 Hz, 3H), 3.21 – 3.15 (m, 4H); ^{13}C NMR (151 MHz, $CDCl_3$) δ 160.63, 154.28, 151.91, 145.75, 130.34, 130.01, 123.93, 123.91, 123.83, 116.51, 116.19, 109.39, 105.45, 103.26, 55.24, 49.44, 45.12; MS (EI, 70 eV) *m/z* (%) 401 (22), 219 (100), 191 (14), 182 (16), 149 (20); purity (HPLC): 99.39 %.

(4-(4-Methoxyphenyl)piperazin-1-yl)(10*H*-phenoxazin-10-yl)methanone (16e). The title compound was prepared from **3a** (2 mmol, 0.36 g) and 1-(4-methoxylphenyl)piperazine (0.38 g, 2 mmol) in 1,2-dichloroethane (20 mL) and pyridine (1 mL) in a similar manner as described for **15g**. Purification by chromatography (ethyl acetate / petroleum ether, 3:7) afforded **16e** as a white powder (0.44 g, 55 %). mp 118-119 °C; FTIR: 1670 cm^{-1} (C=O); ^{1}H NMR (600 MHz, $CDCl_3$) δ 7.03 – 7.00 (m, 2H), 6.94 – 6.84 (m, 10H), 3.78 (s, 3H), 3.76 (t, *J* = 5.0 Hz, 4H), 3.07 (t, *J* = 5.0 Hz, 4H); ^{13}C NMR (151 MHz, $CDCl_3$) δ 154.49, 154.21, 145.61, 145.01, 130.34, 123.91, 123.73, 118.95, 116.48, 116.46, 116.03, 114.55, 55.56, 50.97, 45.38; MS (EI, 70 eV) *m/z* (%) 401 (28), 182 (17), 149 (69); purity (HPLC): 98.57 %.

(4-(4-Chlorophenyl)piperazin-1-yl)(10*H*-phenoxazin-10-yl)methanone (16f). The title compound was prepared from **3a** (2 mmol, 0.36 g) and 1-(4-chlorophenyl)piperazine (0.39 g, 2 mmol) in 1,2-dichloroethane (20 mL) and pyridine (1 mL) in a similar manner as described for **15g**. Purification by chromatography (ethyl acetate / petroleum ether, 3:7) afforded **16f** as a pale yellow powder (0.62 g, 77 %). mp 158-160 °C; FTIR: 1690 cm^{-1} (C=O); ^{1}H NMR (400 MHz, $CDCl_3$) δ 7.24 – 7.18 (m, 2H), 7.03 (ddd, *J* = 5.9, 3.5, 0.6 Hz, 2H), 6.94 – 6.86 (m, 6H), 6.84 – 6.79 (m, 2H), 3.77 – 3.66 (m, 4H), 3.20 – 3.06 (m, 4H); ^{13}C NMR (101 MHz, $CDCl_3$) δ

154.32, 149.18, 145.85, 130.34, 129.15, 125.76, 123.92, 123.89, 117.95, 116.53, 116.30, 49.49, 45.07; MS (APCI) calcd for $C_{23}H_{20}ClN_3O_2$ $[M+H]^+$ 406.1322; found 406.1423; purity HPLC): 99.76 %.

(4-(4-(Trifluoromethyl)phenyl)piperazin-1-yl)(10*H*-phenoxazin-10-yl)methanone (16g). The title compound was prepared from **3a** (2 mmol, 0.36 g) and 1-(4-trifluoromethylphenyl)piperazine (0.46 g, 2 mmol) in 1,2-dichloroethane (20 mL) and pyridine (1 mL) in a similar manner as described for **15g**. Purification by chromatography (ethyl acetate / petroleum ether, 3:7) afforded **16g** as a white powder (0.16 g, 18 %). mp 201-202 °C; FTIR: 1686 cm^{-1} (C=O); ^1H NMR (400 MHz, $CDCl_3$) δ 7.49 (d, J = 8.7 Hz, 2H), 7.10 – 7.02 (m, 2H), 6.96 – 6.86 (m, 8H), 3.76 – 3.69 (m, 4H), 3.32 – 3.24 (m, 4H); ^{13}C NMR (101 MHz, $CDCl_3$) δ 154.42, 152.62, 146.01, 130.35, 128.53, 126.60, 126.56, 126.52, 126.48, 125.83, 124.01, 123.94, 123.14, 121.79, 121.46, 121.13, 116.58, 116.47, 115.15, 48.16, 44.90; MS (EI, 70 eV) *m/z* (%) 439 (18), 257 (100), 215 (12), 214 (10), 183 (12), 182 (51), 172 (12), 145 (15), 70 (36); purity (HPLC): 98.05 %.

(4-(4-Nitrophenyl)piperazin-1-yl)(10*H*-phenoxazin-10-yl)methanone (16h). The title compound was prepared from **3a** (2 mmol, 0.36 g) and 1-(4-nitrophenyl)piperazine (0.41 g, 2 mmol) in 1,2-dichloroethane (20 mL) and pyridine (1 mL) in a similar manner as described for **15g**. Purification by chromatography (ethyl acetate / petroleum ether, 3:7) afforded **16h** as a white powder (0.14 g, 17 %). mp 210-211 °C; FTIR: 1674 cm^{-1} (C=O); ^1H NMR (400 MHz, $CDCl_3$) δ 8.20 – 8.05 (m, 2H), 7.18 – 7.08 (m, 2H), 6.99 – 6.87 (m, 6H), 6.84 – 6.74 (m, 2H), 3.75 – 3.65 (m, 4H), 3.47 – 3.40 (m, 4H); ^{13}C NMR (101 MHz, $CDCl_3$) δ 154.62, 154.21, 146.36, 139.22, 130.34, 126.03, 125.92, 124.26, 124.07, 123.99, 116.85, 116.69, 113.08, 112.32, 46.84, 46.12, 44.65, 29.68; MS (APCI) calcd for $C_{23}H_{21}N_4O_4$ $[M+H]^+$ 417.1653; found 417.1502; purity (HPLC): 95.43 %.

4-(4-(10*H*-Phenoxazine-10-carbonyl)piperazin-1-yl)benzonitrile (16i). The title compound was prepared from **3a** (2 mmol, 0.36 g) and 1-(4-cyanophenyl)piperazine (0.37 g, 2 mmol) in

1,2-dichloroethane (20 mL) and pyridine (1 mL) in a similar manner as described for **15g**. Purification by chromatography (ethyl acetate / petroleum ether, 3:7) afforded **16i** as a white powder (0.44 g, 55 %). mp 197 °C; FTIR: 2207 (CN), 1690 cm^{-1} (C=O); ^{1}H NMR (400 MHz, $CDCl_3$) δ 7.54 – 7.45 (m, 2H), 7.13 – 7.05 (m, 2H), 6.96 – 6.88 (m, 6H), 6.86 – 6.79 (m, 2H), 3.75 – 3.63 (m, 4H), 3.38 – 3.26 (m, 4H); ^{13}C NMR (101 MHz, $CDCl_3$) δ 154.52, 152.73, 146.20, 133.88, 133.59, 130.34, 124.15, 123.96, 119.61, 116.99, 116.68, 116.64, 114.65, 109.99, 101.47, 47.13, 44.73; MS (APCI) calcd for $C_{24}H_{21}N_4O_2$ $[M+H]^+$ 397.1665; found 397.1592; purity (HPLC): 100.00 %.

(2-Chloro-10*H*-phenoxazin-10-yl)(4-(2-methoxyphenyl)piperazin-1-yl)methanone (16j). The title compound was prepared from **3b** (2 mmol, 0.43 g) and 1-(2-methoxyphenyl)piperazine (0.38 g, 2 mmol) in 1,2-dichloroethane (20 mL) and pyridine (1 mL) in a similar manner as described for **15g**. Purification by chromatography (ethyl acetate / petroleum ether, 3:7) afforded **16j** as a white powder (0.49 g, 56%). mp 112 °C; FTIR: 1682 cm^{-1} (C=O); ^{1}H NMR (600 MHz, $CDCl_3$) δ 7.05 (t, J = 4.6 Hz, 2H), 6.95 – 6.81 (m, 8H), 6.76 (d, J = 8.5 Hz, 1H), 3.86 (s, 3H), 3.80 (s, 4H), 3.08 (s, 4H); ^{13}C NMR (151 MHz, $CDCl_3$) δ 153.47, 152.22, 144.99, 143.94, 140.31, 131.21, 129.62, 128.80, 124.14, 123.98, 123.78, 123.09, 121.08, 118.51, 117.13, 116.54, 115.75, 111.33, 55.45, 50.61, 45.50; MS (EI, 70 eV) *m/z* (%) 220 (14), 219 (100), 191 (11), 134 (12); purity (HPLC): 98.99 %.

(2-Chloro-10*H*-phenoxazin-10-yl)(4-(3-methoxyphenyl)piperazin-1-yl)methanone (16k). The title compound was prepared from **3b** (2 mmol, 0.43 g) and 1-(3-methoxyphenyl)piperazine (0.38 g, 2 mmol) in 1,2-dichloroethane (20 mL) and pyridine (1 mL) in a similar manner as described for **15g**. Purification by chromatography (ethyl acetate / petroleum ether, 3:7) afforded **16k** as a white powder (0.20 g, 23%). 78 °C; FTIR: 1670 cm^{-1} (C=O); ^{1}H NMR (600 MHz, $CDCl_3$) δ 7.19 (t, J = 8.4 Hz, 1H), 7.11 (s, 1H), 6.93 – 6.89 (m, 2H), 6.89 – 6.83 (m, 3H), 6.78 (d, J = 8.5 Hz, 1H), 6.58 – 6.53 (m, 1H), 6.49 (d, J = 8.3 Hz, 2H), 3.79 (s, 3H), 3.76 (t, J = 5.2 Hz, 4H), 3.20 (t, J = 5.2 Hz, 4H); ^{13}C NMR (151 MHz,

$CDCl_3$) δ 160.65, 153.61, 145.27, 144.22, 131.19, 130.07, 129.62, 128.83, 124.23, 124.19, 123.33, 117.21, 117.20, 116.66, 116.09, 116.04, 109.55, 105.82, 103.46, 77.23, 77.02, 76.81, 55.27, 49.63, 45.07; MS (EI, 70 eV) *m/z* (%) 435 (10), 220 (13), 219 (100), 216 (11), 150 (10), 149 (14), 1345 (5), 134 (7) ; purity (HPLC): 100 %.

(2,8-Dichloro-10*H*-phenoxazin-10-yl)(4-(2-methoxyphenyl)piperazin-1-yl)methanone (16l). The title compound was prepared from **3c** (2 mmol, 0.50 g) and 1-(2-methoxyphenyl)piperazine (0.38 g, 2 mmol) in 1,2-dichloroethane (20 mL) and pyridine (1 mL) in a similar manner as described for **15g**. Purification by chromatography (ethyl acetate / petroleum ether, 3:7) afforded **16l** as a white powder (0.28 g, 30%). mp 136-137 °C; FTIR: 1668 cm^{-1} (C=O); ^{1}H NMR (400 MHz, $CDCl_3$) δ 7.10 (s, 2H), 6.99 – 6.89 (m, 4H), 6.85 (dd, *J* = 8.5, 2.3 Hz, 2H), 6.76 (d, *J* = 8.5 Hz, 2H), 3.95 – 3.81 (m, 7H), 3.18 (s, br, 4H); ^{13}C NMR (101 MHz, $CDCl_3$) δ 152.87, 152.26, 143.51, 130.43, 129.07, 123.60, 121.25, 117.32, 115.72, 111.61, 55.55, 50.73, 45.17; MS (EI, 70 eV) *m/z* (%) 469 (4), 220 (15), 219 (100), 134 (11), 150 (10), 149 (14); purity (HPLC): 98.77 %.

(2,8-Dichloro-10*H*-phenoxazin-10-yl)(4-(3-methoxyphenyl)piperazin-1-yl)methanone (16m). The title compound was prepared from **3c** (2 mmol, 0.47 g) and 1-(3-methoxyphenyl)piperazine (0.38 g, 2 mmol) in 1,2-dichloroethane (20 mL) and pyridine (1 mL) in a similar manner as described for **15g**. Purification by chromatography (ethyl acetate / petroleum ether, 3:7) afforded **16m** as a white powder (0.59 g, 63%). mp 131 °C; FTIR: 1659 cm^{-1} (C=O); ^{1}H NMR (400 MHz, $CDCl_3$) δ 7.24 – 7.16 (m, 1H), 6.95 (d, *J* = 2.3 Hz, 2H), 6.86 (dd, *J* = 8.5, 2.3 Hz, 2H), 6.77 (d, *J* = 8.5 Hz, 2H), 6.61 – 6.47 (m, 3H), 3.82 – 3.71 (m, 7H; *three of them to* s, 3.79, 3H), 3.25 – 3.19 (m, 4H); ^{13}C NMR (101 MHz, $CDCl_3$) δ 160.66, 160.65, 152.93, 143.70, 130.45, 130.11, 129.09, 123.72, 117.37, 115.92, 109.70, 106.31, 103.66, 55.27, 49.81, 45.06, 43.43; MS (EI, 70 eV) *m/z* (%) 471 (5), 470 (2), 469 (7), 220 (16), 219 (100), 150 (12), 149 (18), 148 (9); purity (HPLC): 99.50 %.

10-(4-(2-Methoxyphenyl)piperazine-1-carbonyl)-10*H*-phenoxazine-3-carbonitrile (16n). The title compound was prepared from **3d** (2 mmol, 0.47 g) and 1-(2-methoxyphenyl)piperazine (0.38 g, 2 mmol) in 1,2-dichloroethane (20 mL) and pyridine (1 mL) in a similar manner as described for **15g**. Purification by chromatography (ethyl acetate / petroleum ether, 3:7) afforded **16n** as a white powder (0.52 g, 61%). mp 188 °C; FTIR: 2214 (CN), 1686 cm^{-1} (C=O); ^{1}H NMR (400 MHz, $CDCl_3$) δ 7.28 – 7.23 (m, 1H), 7.17 (dd, *J* = 8.4, 1.9 Hz, 1H), 7.10 – 7.04 (m, 1H), 7.03 (d, *J* = 1.8 Hz, 1H), 6.96 – 6.87 (m, 5H), 6.85 – 6.80 (m, 1H), 6.75 – 6.69 (m, 1H), 3.90 – 3.79 (m, 7H), 3.11 (s, 4H); ^{13}C NMR (101 MHz, $CDCl_3$) δ 152.38, 152.19, 144.69, 143.92, 134.52, 128.79, 128.69, 124.56, 124.46, 121.11, 119.31, 118.39, 116.67, 114.97, 114.89, 111.46, 105.94, 55.46, 50.67, 45.40; MS (EI, 70 eV) *m/z* (%) 427 (3), 426 (8), 220 (14), 219 (100), 134 (17), 120 (14), 86 (11), 84 (15); purity (HPLC): 98.89 %.

10-(4-(3-Methoxyphenyl)piperazine-1-carbonyl)-10*H*-phenoxazine-3-carbonitrile (16o). The title compound was prepared from **3d** (2 mmol, 0.41 g) and 1-(3-methoxyphenyl)piperazine (0.38 g, 2 mmol) in 1,2-dichloroethane (20 mL) and pyridine (1 mL) in a similar manner as described for **15g**. Purification by chromatography (ethyl acetate / petroleum ether, 3:7) afforded **16o** as a white powder (0.44 g, 52%). mp 167 °C; FTIR: 2222 (CN), 1682 cm^{-1} (C=O); ^{1}H NMR (600 MHz, $CDCl_3$) δ 7.19 (td, *J* = 8.2, 0.7 Hz, 1H), 7.17 (ddd, *J* = 8.4, 1.9, 0.8 Hz, 1H), 7.04 (dd, *J* = 1.9, 0.7 Hz, 1H), 6.94 – 6.88 (m, 3H), 6.86 – 6.82 (m, 1H), 6.73 – 6.69 (m, 1H), 6.52 (dd, *J* = 8.3, 2.3 Hz, 1H), 6.49 (dd, *J* = 8.1, 2.3 Hz, 1H), 6.45 (d, *J* = 2.4 Hz, 1H), 3.83 – 3.74 (m, 7H), 3.21 (t, *J* = 5.2 Hz, 4H); ^{13}C NMR (151 MHz, $CDCl_3$) 160.66, 152.42, 151.69, 144.83, 144.04, 134.51, 130.09, 128.81, 128.71, 128.70, 124.60, 124.58, 119.39, 118.37, 116.77, 115.08, 115.04, 109.47, 106.11, 105.69, 103.46, 55.26, 49.57, 45.11; MS (APCI) calcd for $C_{25}H_{23}N_4O_3$ $[M+H]^+$ 427.1770; found 427.1786; purity (HPLC): 99.40 %.

10-(4-(4-Methoxyphenyl)piperazine-1-carbonyl)-10*H*-phenoxazine-3-carbonitrile (16p). The title compound was prepared from **3d** (2 mmol, 0.42 g) and 1-(4-methoxyphenyl)piperazine (0.38 g, 2 mmol) in 1,2-dichloroethane (20 mL) and pyridine (1 mL) in a similar manner as described for **15g**. Purification by chromatography (ethyl acetate / petroleum ether, 1:1) afforded **16p** as a white powder (0.23 g, 27%). mp 171 °C; FTIR: 1678 cm^{-1} (C=O); ^{1}H NMR (400 MHz, $CDCl_3$) δ 7.17 (ddd, *J* = 8.4, 1.9, 0.5 Hz, 1H), 7.04 (dd, *J* = 1.8, 0.6 Hz, 1H), 6.94 – 6.88 (m, 5H), 6.87 – 6.82 (m, 3H), 6.74 – 6.68 (m, 1H), 3.81 (t, *J* = 4.9 Hz, 4H), 3.77 (s, 3H), 3.09 (t, *J* = 5.1 Hz, 4H); ^{13}C NMR (101 MHz, $CDCl_3$) δ 152.39, 144.78, 144.00, 134.51, 128.79, 128.70, 124.57, 124.54, 119.36, 119.15, 118.36, 116.72, 115.04, 114.61, 109.99, 106.05, 55.55, 51.17, 45.31; MS (APCI) calcd for $C_{25}H_{23}N_4O_3$ $[M+H]^+$ 427.1770; found 427.1811; purity (HPLC): 99.40 %.

(5*H*-Dibenzo[*b*,*f*]azepin-5-yl)(4-(2-methoxyphenyl)piperazin-1-yl)methanone (17a). The title compound was prepared from **9** (2 mmol, 0.47 g) and 1-(2-methoxyphenyl)piperazine (0.38 g, 2 mmol) in 1,2-dichloroethane (20 mL) and pyridine (1 mL) in a similar manner as described for **15g**. Purification by chromatography (ethyl acetate / petroleum ether, 1:1) afforded **17a** as a white powder (0.30 g, 37%). mp 188-189 °C; FTIR: 1647 cm^{-1} (C=O); ^{1}H NMR (600 MHz, $CDCl_3$) δ 7.59 (dd, *J* = 8.1, 1.2 Hz, 2H), 7.38 (ddd, *J* = 8.3, 7.2, 1.7 Hz, 2H), 7.28 – 7.23 (m, 2H), 7.22 (td, *J* = 7.4, 1.3 Hz, 2H), 7.00 – 6.96 (m, 1H), 6.95 (s, 2H), 6.87 (td, *J* = 7.6, 1.4 Hz, 1H), 6.84 – 6.77 (m, 2H), 3.81 (s, 3H), 3.36 – 3.23 (m, 4H), 2.88 – 2.60 (m, 4H); ^{13}C NMR (151 MHz, $CDCl_3$) δ 218.62, 159.13, 152.13, 142.78, 140.95, 134.08, 131.32, 131.32, 129.04, 128.87, 127.63, 126.34, 123.16, 120.94, 118.22, 111.18, 55.36, 50.18, 46.15; MS (APCI) calcd for $C_{25}H_{26}N_3O_3$ $[M+H]^+$ 412.2025; found 412.2060; purity (HPLC): 100.00 %.

(5*H*-Dibenzo[*b*,*f*]azepin-5-yl)(4-(3-methoxyphenyl)piperazin-1-yl)methanone (17b). The title compound was prepared from **9** (2 mmol, 0.39 g) and 1-(3-methoxyphenyl)piperazine (0.38 g, 2 mmol) in 1,2-dichloroethane (20 mL) and pyridine (1 mL) in a similar manner as

described for **15g**. Purification by chromatography (ethyl acetate / petroleum ether, 1:1) afforded **17b** as a white powder (0.18 g, 22 %). mp 112-113 °C; FTIR: 1647 cm^{-1} (C=O); ^{1}H NMR (400 MHz, $CDCl_3$) δ 7.57 (dd, *J* = 8.0, 1.2 Hz, 2H), 7.38 (ddd, *J* = 7.8, 7.0, 1.8 Hz, 2H), 7.30 – 7.19 (m, 4H), 7.13 (s, 1H), 6.96 (s, 2H), 6.41 (s, 3H), 3.76 (s, 3H), 3.27 (s, br, 4H), 2.90 (s, br, 4H); ^{13}C NMR (101 MHz, $CDCl_3$) δ 160.53, 159.11, 142.54, 134.06, 131.28, 129.79, 129.08, 128.89, 127.63, 126.45, 108.89, 104.65, 102.60, 55.18, 48.55, 45.79, 31.58, 14.11; MS (EI, 70 eV) *m/z* (%) 412 (20), 411 (63), 263 (5), 262 (19), 250 (5), 259 (23), 221 (6), 220 (36), 219 (72), 194 (9), 193 (45), 192 (100), 191 (37), 190 (212), 189 (5), 177 (9), 176 (11), 175 (42), 165 (21), 164 (10), 163 (47), 162 (45); purity (HPLC): 100.00 %.

(10,11-Dihydro-5*H*-dibenzo[*b*,*f*]azepin-5-yl)(4-(2-methoxyphenyl)piperazin-1-yl)methanone (18). The title compound was prepared from **10** (2 mmol, 0.39 g) and 1-(2-methoxyphenyl)piperazine (0.38 g, 2 mmol) in 1,2-dichloroethane (20 mL) and pyridine (1 mL) in a similar manner as described for **15g**. Purification by chromatography (ethyl acetate / petroleum ether, 1:1) afforded **18** as a white powder (0.22 g, 27%). mp 188-189 °C; FTIR: 1643 cm^{-1} (C=O); ^{1}H NMR (400 MHz, $CDCl_3$) δ 7.47 (s, 2H), 7.21 – 7.09 (m, 6H), 7.03 – 6.95 (m, 1H), 6.93 – 6.81 (m, 3H), 3.83 (s, 3H), 3.52 (s, br, 4H), 3.17 (s, 4H), 2.90 (s, br, 4H); ^{13}C NMR (101 MHz, $CDCl_3$) δ 158.66, 152.16, 143.04, 134.98, 129.85, 127.52, 126.69, 126.59, 123.22, 121.00, 118.27, 111.25, 55.37, 50.30, 46.22, 31.02; MS (EI, 70 eV) *m/z* (%) 414 (27), 413 (93), 219 (100), 195 (26), 194 (59), 193 (22), 1902 (13), 191 (21), 134 (49); purity (HPLC): 100.00 %.

4-(3-Methoxyphenyl)-*N*,*N*-diphenylpiperazine-1-carboxamide (19). The title compound was prepared from **12** (2 mmol, 0.34 g) and 1-(3-methoxyphenyl)piperazine (0.38 g, 2 mmol) in 1,2-dichloroethane (20 mL) and pyridine (1 mL) in a similar manner as described for **15g**. Purification by chromatography (ethyl acetate / petroleum ether, 3:7) afforded **19** as a white powder (46 mg, 6 %). mp 97-98 °C; FTIR: 1655 cm^{-1} (C=O); ^{1}H NMR (400 MHz, $CDCl_3$) δ 7.36 – 7.28 (m, 4H), 7.20 – 7.11 (m, 3H), 7.10 – 7.03 (m, 4H), 6.52 – 6.40 (m, 3H), 3.78 (s,

3H), 3.54 (t, J = 5.0 Hz, 4H), 3.05 (t, J = 5.1 Hz, 4H); ^{13}C NMR (101 MHz, $CDCl_3$) δ 160.58, 159.69, 144.80, 129.90, 129.29, 125.19, 124.92, 109.22, 103.01, 55.20, 49.06, 45.34; MS (APCI) calcd for $C_{24}H_{25}N_3O_2$ $[M+H]^+$ 388.2025, found 388.1996; purity (HPLC): 100.00 %.

4-(2-Methoxyphenyl)-*N*-(2-phenoxyphenyl)piperazine-1-carboxamide (20a). The title compound was prepared from 2-phenoxyaniline (**13**, 0.37 g, 2.0 mmol) and 1-(2-methoxyphenyl)piperazine (0.38 g, 2.0 mmol) in a similar manner as described for **15g**. The crude product was purified by column chromatography (petroleum ether / ethyl acetate, 6:4) to afford **20a** as a colorless oil (0.26 g, 32%). FTIR 1663 cm^{-1} (C=O); ^{1}H NMR (400 MHz, $CDCl_3$) δ 8.26 (dd, J = 1.5, 8.2 Hz, 1H, N*H*), 7.38 – 7.32 (m, 2H, *H*-Ar), 7.16 – 7.10 (m, 2H, *H*-Ar), 7.07 – 7.00 (m, 4H, *H*-Ar), 6.98 – 6.85 (m, 5H, *H*-Ar), 3.87 (s, 3H, OCH_3), 3.61 (s, br, 4H, NCH_2), 3.04 (s, br, 4H, NCH_2). ^{13}C NMR (151 MHz, $CDCl_3$) δ 156.83, 154.57, 152.38, 145.15, 131.23, 130.12, 124.58, 123.83, 122.67, 121.20, 120.50, 118.36, 118.27, 55.59, 50.61, 44.35; MS (APCI) calcd for $C_{24}H_{25}N_3O_3$ $[M+H]^+$ 404.1974, found 404.2052; purity (HPLC) 99.74%.

4-(3-Methoxyphenyl)-*N*-(2-phenoxyphenyl)piperazine-1-carboxamide (20b). The title compound was prepared from 2-phenoxyaniline (**13**, 0.37 g, 2.0 mmol) and 1-(3-methoxyphenyl)piperazine (0.38 g, 2.0 mmol) in a similar manner as described for **15g**. The crude product was purified by column chromatography (petroleum ether / ethyl acetate, 6:4) to afford **20b** as a colorless oil (0.38 g, 47%). FTIR 1647 cm^{-1} (C=O); ^{1}H NMR (400 MHz, $CDCl_3$) δ 8.24 (dd, J = 1.5, 8.2 Hz, 1H, N*H*), 7.38 – 7.32 (m, 2H, *H*-Ar), 7.16 – 7.10 (m, 2H, *H*-Ar), 7.05 – 7.00 (m, 3H, *H*-Ar), 6.99 – 6.93 (m, 1H, *H*-Ar), 6.92 – 6.82 (m, 5H, *H*-Ar), 3.77 (s, 3H, OCH_3), 3.58 (s, br, 4H, NCH_2), 3.07 – 3.01 (m, 4H, NCH_2). ^{13}C NMR (101 MHz, $CDCl_3$) δ 156.84, 154.50, 145.11, 131.16, 130.14, 124.64, 123.83, 122.80, 120.57, 118.49, 118.17, 114.71, 55.71, 50.91, 44.19; MS (APCI) calcd for $C_{24}H_{25}N_3O_3$ $[M+H]^+$ 404.1974, found 404.2016; purity (HPLC) 99.50%.

4-(4-Methoxyphenyl)-*N*-(2-phenoxyphenyl)piperazine-1-carboxamide (20c). The title compound was prepared from 2-phenoxyaniline (**13**, 0.37 g, 2.0 mmol) and 1-(4-methoxyphenyl)piperazine (0.38 g, 2.0 mmol) in a similar manner as described for **15g**. The crude product was purified by column chromatography (petroleum ether / ethyl acetate, 6:4) to afford **20c** as a white powder (0.50 g, 62%). mp 106 °C; FTIR 1659 cm^{-1} (C=O); ^{1}H NMR (400 MHz, $CDCl_3$) δ 8.24 (dd, *J* = 1.5, 8.2 Hz, 1H, N*H*), 7.38 – 7.32 (m, 2H, *H*-Ar), 7.16 – 7.10 (m, 2H, *H*-Ar), 7.05 – 7.00 (m, 3H, *H*-Ar), 6.99 – 6.93 (m, 1H, *H*-Ar), 6.92 – 6.82 (m, 5H, *H*-Ar), 3.77 (s, 3H, OCH_3), 3.58 (s, br, 4H, NCH_2), 3.07 – 3.01 (m, 4H, NCH_2). ^{13}C NMR (101 MHz, $CDCl_3$) δ 156.84, 154.50, 145.11, 131.16, 130.14, 124.64, 123.83, 122.80, 120.57, 118.49, 118.17, 114.71, 55.71, 50.91, 44.19; MS (APCI) calcd for $C_{24}H_{25}N_3O_3$ $[M+H]^+$ 404.1974, found 404.1979; purity (HPLC) 100.00%.

***N*-(4-Methoxyphenyl)-10*H*-phenoxazine-10-carboxamide (21).** The title compound was prepared from **3a** (2 mmol, 0.36 g) and 4-methoxyaniline (0.25 g, 2 mmol) in 1,2-dichloroethane (20 mL) and pyridine (1 mL) in a similar manner as described for **15g**. Purification by chromatography (ethyl acetate / petroleum ether, 3:7) afforded **21** as a white powder (86 mg, 13%). mp 127 °C; FTIR: 1655 cm^{-1} (C=O); ^{1}H NMR (400 MHz, $CDCl_3$) δ 7.65 – 7.59 (m, 2H), 7.34 – 7.27 (m, 2H), 7.22 – 7.09 (m, 7H), 6.87 – 6.81 (m, 2H), 3.78 (s, 3H); ^{13}C NMR (101 MHz, $CDCl_3$) δ 156.35, 152.19, 151.29, 130.70, 129.23, 126.68, 124.38, 124.36, 123.87, 122.11, 117.24, 114.18, 55.49; MS (EI, 70 eV) *m/z* (%) 333 (2), 332 (7), 184 (13), 183 (100), 182 (13), 154 (13), 154 (8), 149 (9); purity (HPLC): 97.42 %.

***N*-(3-Methoxybenzyl)-10*H*-phenoxazine-10-carboxamide (22a).** The title compound was prepared from **3a** (2 mmol, 0.36 g) and 3-methoxybenzylamine (0.27 g, 2 mmol) in 1,2-dichloroethane (20 mL) and pyridine (1 mL) in a similar manner as described for **15g**. Purification by chromatography (ethyl acetate / petroleum ether, 3:7) afforded **22a** as a white powder (0.28 g, 40%). mp 114 °C; FTIR: 1659 cm^{-1} (C=O); ^{1}H NMR (400 MHz, $CDCl_3$) δ 7.57 – 7.50 (m, 2H), 7.28 – 7.21 (m, 2H), 7.18 – 7.05 (m, 5H), 6.91 – 6.87 (m, 1H), 6.85 –

6.79 (m, 2H), 4.46 (d, J = 5.6 Hz, 2H), 3.80 (s, 3H); ^{13}C NMR (101 MHz, $CDCl_3$) 159.86, 154.56, 151.27, 140.03, 129.75, 129.35, 126.46, 124.49, 123.75, 119.83, 117.12, 113.23, 112.89, 109.99, 55.23, 44.90; MS (EI, 70 eV) *m/z* (%) 347 (1), 346 (5), 184 (16), 183 (100), 182 (31), 154 (11), 121 (8); purity (HPLC): 98.90 %.

***N*-(4-Methoxybenzyl)-10*H*-phenoxazine-10-carboxamide (22b).** The title compound was prepared from **3a** (2 mmol, 0.47 g) and 4-methoxybenzylamine (0.27 g, 2 mmol) in 1,2-dichloroethane (20 mL) and pyridine (1 mL) in a similar manner as described for **15g**. Purification by chromatography (ethyl acetate / petroleum ether, 3:7) afforded **22b** as a white powder (0.12 g, 17 %). mp 129 °C; FTIR: 1659 cm^{-1} (C=O); ^{1}H NMR (600 MHz, $CDCl_3$) δ 7.53 (dd, J = 7.8, 1.6 Hz, 2H), 7.25 – 7.20 (m, 2H), 7.15 – 7.04 (m, 6H), 6.88 – 6.84 (m, 2H), 4.41 (d, J = 5.5 Hz, 2H), 3.79 (s, 3H); ^{13}C NMR (151 MHz, $CDCl_3$) δ 218.59, 154.52, 151.25, 130.54, 130.52, 129.40, 129.07, 129.06, 126.47, 126.41, 124.48, 123.75, 117.11, 114.13, 114.08, 55.30, 44.45; MS (EI, 70 eV) *m/z* (%) 346 (6), 184 (12), 183 (100), 182 (12), 121 (19); purity (HPLC): 99.86 %.

2-(4-(2-Methoxyphenyl)piperazin-1-yl)-1-(10*H*-phenoxazin-10-yl)ethan-1-one (24a). The title compound was prepared from a mixture of **23**[24] (4 mmol, 1.04 g), 1-(2-methoxyphenyl)piperazine (0.77 g, 4 mmol) and dry K_2CO_3 (0.68 g, 4.2 mmol) in acetonitrile (20 mL) under reflux. Purification by chromatography (ethyl acetate / petroleum ether, 3:7) afforded **24a** as a white powder (0.28 g, 17%). mp 131-132 °C; FTIR: 1670 cm^{-1} (C=O; ^{1}H NMR (600 MHz, $CDCl_3$) δ 7.67 – 7.57 (m, 2H), 7.23 – 7.17 (m, 2H), 7.16 – 7.10 (m, 4H), 6.99 (ddd, J = 8.0, 6.4, 2.6 Hz, 1H), 6.94 – 6.88 (m, 2H), 6.86 – 6.81 (m, 1H), 3.84 (s, 3H), 3.48 (s, 2H), 3.07 (s, 4H), 2.75 (s, 4H); ^{13}C NMR (151 MHz, $CDCl_3$) δ 168.40, 152.24, 151.08, 151.07, 141.19, 129.34, 127.02, 124.93, 123.40, 123.38, 122.95, 120.98, 118.25, 116.89, 111.25, 59.99, 55.36, 53.31, 50.48; ; MS (APCI) calcd for $C_{25}H_{26}N_3O_3$ $[M+H]^+$ 416.1974; found 416.1963; purity (HPLC): 100.00 %.

2-(4-(3-Methoxyphenyl)piperazin-1-yl)-1-(10*H*-phenoxazin-10-yl)ethan-1-one (24b). The title compound was prepared from a mixture of **23** (4 mmol, 1.04 g), 1-(3-methoxyphenyl)piperazine (0.77 g, 4 mmol) and dry K_2CO_3 (0.68 g, 4.2 mmol) in acetonitrile (20 mL) as described for **24a**. Purification by chromatography (ethyl acetate / petroleum ether, 3:7) afforded **24b** as a white powder (0.89 g, 54%). mp 124 °C; FTIR: 1659 cm^{-1} (C=O); ^{1}H NMR (400 MHz, $CDCl_3$) δ 7.61 (dd, *J* = 8.2, 1.6 Hz, 2H), 7.24 – 7.17 (m, 2H), 7.16 – 7.09 (m, 5H), 6.52 (ddd, *J* = 8.3, 2.4, 0.8 Hz, 1H), 6.45 – 6.37 (m, 2H), 3.78 (s, 3H), 3.48 (s, 2H), 3.20 – 3.12 (m, 4H), 2.74 – 2.64 (m, 4H); ^{13}C NMR (101 MHz, $CDCl_3$) 168.24, 160.55, 152.49, 151.06, 129.75, 129.26, 127.06, 124.85, 123.40, 116.92, 108.88, 104.50, 102.55, 59.87, 55.17, 52.89, 48.94, 15.26; MS (EI, 70 eV) *m/z* (%) 416 (4), 415 (12), 207 (4), 206 (38), 205 (100), 190 (27), 183 (12), 182 (33), 162 (30), 134 (13); purity (HPLC): 100.00 %. purity (HPLC): 100.00 %.

9-(4-Phenylpiperazin-1-yl)acridine (27a). The title compound was prepared from 1-phenylpiperazine (0.32 g, 2 mmol) in a similar manner as described for **27d**. Purification by chromatography (petroleum ether/ethyl acetate, 6:4) afforded **27a** as a yellow powder (0.26 g, 26%). mp 188 °C; FTIR: 1631 cm^{-1}(C=C), 1415 cm^{-1}(C–H); ^{1}H NMR (400 MHz, $CDCl_3$) δ 8.44 (d, *J* = 8.7 Hz, 2H), 8.27 (d, *J* = 8.7 Hz, 2H), 7.79 – 7.72 (m, 2H), 7.54 – 7.47 (m, 2H), 7.38 – 7.32 (m, 2H), 7.09 (d, *J* = 7.9 Hz, 2H), 6.96 (t, *J* = 7.3 Hz, 1H), 3.86 (t, 4H), 3.54 (t, 4H);^{13}C NMR (101 MHz, $CDCl_3$) δ 151.79, 150.20, 150.19, 133.46, 130.15, 129.43, 127.32, 125.03, 124.82, 124.52, 121.52, 120.59, 116.93, 116.65, 53.02, 51.12; MS (APCI) calcd for $C_{23}H_{21}N_3$ $[M+H]^+$ 340.1813, found 340.1854; purity (HPLC) 96.06%.

9-(4-(2-Methoxyphenyl)piperazin-1-yl)acridine (27b). The title compound was prepared from 1-(2-methoxyphenyl)piperazine (0.38 g, 2 mmol) in a similar manner as described for **27d**. Purification by chromatography (petroleum ether/ethyl acetate 6:4) afforded **27b** as a yellow powder (0.57 g, 77%). mp 178 °C; FTIR: 2981 cm^{-1} (OCH_3),1520 cm^{-1} (C=C); ^{1}H NMR (600 MHz, $CDCl_3$) δ 8.48 (d, *J* = 8.7 Hz, 2H), 8.29 (d, *J* = 6.9 Hz, 2H), 7.78 – 7.74 (m,

2H), 7.53 – 7.48 (m, 2H), 7.13 – 7.07 (m, 2H), 7.01 (td, *J* = 1.4, 7.6 Hz, 1H), 6.95 (dd, *J* = 1.3, 8.0 Hz, 1H), 3.95 (s, br, 3H), 3.91 (s, 4H), 3.43 (t, 4H); ^{13}C NMR (151 MHz, $CDCl_3$) δ 152.53, 141.46, 125.07, 124.92, 123.60, 121.25, 118.67, 111.51, 55.63, 53.51, 52.27; MS (APCI) calcd for $C_{24}H_{23}N_3O$ $[M+H]^+$ 370.1919, found 370.1974; purity (HPLC) 98.39%.

9-(4-(3-Methoxyphenyl)piperazin-1-yl)acridine (27c). The compound was prepared in a similar manner as described for **27d** using 1-(4-methoxyphenyl)piperazine (0.38 g, 2 mmol) in 1,2 dichlorethane. Purification by chromatography (petroleum ether/ethyl acetate, 6:4) afforded **27c** as an orange powder (0.29 g, 40%). mp 184 °C; FTIR: 2823 cm^{-1} (OCH_3), 1600 cm^{-1} (C=C); ^{1}H NMR (400 MHz, $CDCl_3$) δ 8.41 (d, *J* = 8.7 Hz, 3H), 7.80 (t, 2H), 7.53 (t, 2H), 7.27 (t, *J* = 8.2 Hz, 2H), 6.70 (dd, *J* = 8.2, 1.9 Hz, 1H), 6.62 (t, *J* = 2.3 Hz, 1H), 6.53 (dd, *J* = 8.1, 2.2 Hz, 1H), 3.95 (s, br, 4H), 3.85 (s, 3H), 3.56 (t, 4H); ^{13}C NMR (101 MHz, $CDCl_3$) δ 160.86, 153.13, 130.12, 125.08, 124.84, 110.17, 109.62, 105.32, 103.40, 55.42, 53.08, 51.01; MS (APCI) calcd for $C_{24}H_{23}N_3O$ $[M+H]^+$ 370.1919, found 370.1986; purity (HPLC) 99.21%.

9-(4-(4-Methoxyphenyl)piperazin-1-yl)acridine (27d). To acridone (**11**, 0.39 g, 2 mmol) in 1,2 dichloroethane (20 mL) was added bis(trichloromethyl) carbonate (0.36 g, 1.2 mmol) and pyridine (1 mL). The mixture was heated to 75 °C for 1 h and stirred under nitrogen. After 1 h (TLC control, SiO_2, petroleum ether/ ethyl acetate 6:4) 1-(4-methoxyphenyl)piperazine (0.38 g, 2 mmol) was added and the resulting mixture was stirred and refluxed for 2 h. The reaction mixture was cooled, quenched with aequeous HCl (20 mL, 0.5 M) and extracted with CH_2Cl_2 (3 × 20 mL). The combined organic phase was washed with water, dried over Na_2SO_4, concentrated, and purified by chromatography (petroleum ether/ ethyl acetate, 6:4) to provide **27d** as a yellow powder (0.28 g, 38%). mp 186 °C dec.; FTIR: 2816 cm^{-1} (OCH_3), 1508 cm^{-1} (C=C); ^{1}H NMR (400 MHz, $CDCl_3$) δ 8.42 (d, *J* = 8.9 Hz, 4H), 7.81 (t, *J* = 7.4 Hz, 2H), 7.57 – 7.48 (m, 2H), 7.07 (d, *J* = 2.1 Hz, 2H), 6.95 – 6.89 (m, 2H), 3.97 (s, 4H), 3.82 (s, 3H), 3.48 – 3.42 (m, 4H); ^{13}C NMR (151 MHz, $CDCl_3$) δ 154.60, 145.86, 133.04, 127.04, 126.84,

125.13, 125.02, 123.72, 121.54, 119.14, 116.41, 113.31, 55.88, 55.76, 52.48; MS (APCI) calcd for $C_{24}H_{23}N_3O$ $[M+H]^+$ 370.1919, found 370.1917; purity (HPLC) 95.92%.

9-(4-(4-Methylphenyl)piperazin-1-yl)acridine (27e). The compound was prepared from 1-(4-methylphenyl)piperazine (0.38 g, 2 mmol) in a similar manner as described for **27d.** Purification by chromatography (CH_2Cl_2/ ethyl acetate, 3:1) afforded **27e** as a yellow powder (0.3 g, 42%). mp 196 °C; FTIR: 2804 cm^{-1} (CH_3), 1508 cm^{-1} (C=C); ^1H NMR (400 MHz, $CDCl_3$) δ 8.44 (d, *J* = 8.3 Hz, 2H), 8.25 (d, *J* = 8.7 Hz, 2H), 7.78 – 7.71 (m, 2H), 7.53 – 7.46 (m, 2H), 7.16 (d, *J* = 8.4 Hz, 2H), 7.00 (d, *J* = 8.5 Hz, 2H), 3.84 (t, 4H), 3.48 (t, 4H), 2.33 (s, 3H); ^{13}C NMR (101 MHz, $CDCl_3$) δ 150.22, 149.69, 130.16, 129.95, 124.99, 124.86, 124.52, 117.25, 53.07, 51.65, 20.65. MS (APCI) calcd for $C_{24}H_{23}N_3$ $[M+H]^+$ 354.1970, found 354.1984; purity (HPLC) 97.71%.

9-(4-(4-Nitrophenyl)piperazin-1-yl)acridine (27f).[2] The compound was prepared from 1-(4-nitrophenyl)piperazine (0.41 g, 2 mmol) in the same manner as described for **27d**. The crude product was purified by chromatography (CH_2Cl_2/ ethyl acetate, 3:1) and afforded **27f** as an orange powder (0.27 g, 35%). mp 268 °C dec.; FTIR: 1589 cm^{-1} (C=C), 1481 cm^{-1} (NO_2); ^1H NMR (400 MHz, $CDCl_3$) δ 8.38 (d, *J* = 8.8 Hz, 2H), 8.33 (d, *J* = 9.5 Hz, 2H), 8.21 (d, *J* = 9.4 Hz, 2H), 7.79 (t, 2H), 7.53 (t, 2H), 7.00 (d, *J* = 9.4 Hz, 2H), 3.86 (s, br, 4H), 3.80 (t, 4H); ^{13}C NMR (101 MHz, $CDCl_3$) δ 155.26, 150.09, 139.22, 130.32, 130.24, 126.17, 125.48, 124.53, 124.40, 52.30, 48.90; MS (APCI) calcd for $C_{23}H_{20}N_4O_2$ $[M+H]^+$ 385.1664, found 385.1672; purity (HPLC) 97.90%.

Acridin-9-yl benzoate (28). Benzoyl chloride (0.32 mL, 2.8 mmol) was added to a suspension of **11** (0.39 g, 2 mmol) and triethylamine (0.41 mL, 3 mmol) in 1,2 dichloroethane (15 mL) at 0 °C under nitrogen. To the resulting suspension was added pyridine (0.24 mL, 3 mmol). The mixture was stirred and refluxed for 3 h. The reaction was cooled, quenched with an aqueous HCl solution (20 mL, 0.5 M) and extracted with CH_2Cl_2 (3 × 20 mL). The combined organic layers were dried over Na_2SO_4 and concentrated under reduced pressure.

Purification of the residue (ethyl acetate/petroleum ether, 3:7) afforded **28** as yellow crystals (0.9 g, 76%). mp 211 °C; FTIR: 1728 cm^{-1} ;^{1}H NMR (400 MHz, $CDCl_3$) δ 8.44 (dd, J = 0.95, 8.16 Hz, 2H), 8.30 (d, J = 8.84 Hz, 2H), 8.07 – 8.01 (m, 2H), 7.86 – 7.75 (m, 3H), 7.65 (t, 2H), 7.55 (ddd, J = 0.87, 6.59, 8.66 Hz, 2H); ^{13}C NMR (101 MHz, $CDCl_3$) δ 164.49, 149.88, 134.69, 130.83, 129.62, 129.22, 128.29, 126.61, 121.96, 119.93; MS(APCI) calcd for $C_{20}H_{13}NO_2[M+H]^+$ 300.1023, found 300.1019; purity (HPLC) 98.85%.

Biological Assay Methods

Cells and Culture Conditions. Human chronic myelogenous K562 leukemia cells were obtained from DSMZ, Braunschweig, Germany, and cultured at 37 °C under 5% CO_2 in RPMI 1640 medium (Gibco) containing 10% fetal bovine serum (FBS, Biochrom KG), streptomycin (0.1 mg/mL), penicillin G (100 units/mL), and L-glutamine (30 mg/L). The cell line was confirmed as mycoplasma negative using MycoAlert™ (Lonza, Basel) mycoplasma detection kit, and then the assay was performed as described previously.[47]

Cell-based compound screening utilizing a panel of 93 tumour cell lines by means of sulforhodamine B staining was performed by following the protocol described by DTP NCI (http://dtp.nci.nih.gov/branches/btb/ivclsp.html) and in full detail specific for this study in the SI.

Assay of Cell Growth. Growth inhibitory properties were performed using a K562 cancer cell line model as previously described in full detail.[13]

Isolation of MTP and In Vitro MT Assembly Assay by Turbidimetric Measurement. Isolation of microtubule protein (MTP) consisting and performance the MT assembly assay and turbidimetric measurement were performed as previously described in full detail.[13]

EBI Competition Assay. K562 cells were plated at 2 × 10^6 cells/mL in 24 well dishes (Costar, Cambridge, MA). Control wells received equal volumes (1.25 μL, 0.25 %) of vehicle alone and test compounds were made soluble in DMSO. Cells were first incubated with

compounds (equal volumes of 1.25 μL) **15b** (40 and 20 μM), **16n** (14 and 7 μM), vinblastine (5 μM), and colchicine (5 μM) for 2 h. This was followed by treatment with EBI (100 μM) for 1.5 h. The final volume in the well was 500 μL. The cells were harvested, washed with PBS (1 mL) and thereafter resuspended in lysis buffer (5mM Hepes pH 7,5, 150 mM NaCl, 1% deoxycholate, 1% Nonidet P40 0.1 %, + protease inhibitor cOmplete ULTRA Tablet, Mini, EDTA-free, EASYpack, Roche) for 20 min on ice. After centrifugation at 13,000 rpm for 20 min at 4 °C, supernatants were transferred to new Eppendorf tubes. Protein concentrations were determined by Bradford assay and cell extracts were prepared for Western blot analysis. The protein (20 μg/μL) was mixed with an equal volume of SDS-PAGE sample buffer [2× sample buffer: 500 mM Tris-HCl (pH 6.8), 50% (m/v) glycerol, 10% SDS, bromophenol blue 1%, 50 μL/mL 2-mercaptoethanol], heated for 5 min at 95 °C and thereafter subjected to gel electrophoresis (Mini-PROTEAN® TGX™ Precast Gels, 4-15% gradient gel). Protein cell lysates were transferred onto nitrocellulose membranes (0.45 μM, Bio-Rad laboratories, cat. 162-0145), blocked with 5% non-fat dry milk powder in TBS-Tween for 1 h, followed by incubation with primary anti-β-tubulin antibody (abcam, anti-beta tubulin antibody ab15568, diluted with 3% non-fat dry milk powder in TBS-Tween) for 16 h at 4 °C. Membranes were washed several times with TBS-Tween before probed with the secondary horseradish-peroxidase linked anti-rabbit IgG (Goat Anti-Rabbit IgG HRP, Jackson ImmunoResearch Inc., Westgrove, USA), diluted in 3% nonfat dry milk powder TBS-Tween, for 45 min at RT. Immunoreactive proteins were then visualized by the Western blot enhanced chemiluminescent staining using ECL reagents (Clarity™ Western ECL Substrate Bio-Rad laboratories).

Flow Cytometric Analysis of Cell-Cycle Status. Analysis of cell cycle status was carried out as described previously in full detail.[13]

Docking, CoMFA and CoMSIA Studies. Data set. Molecular docking studies were performed as previously described in full detail.[41] Docking and 3D-QSAR analyses were

carried out using a collection of 19 compounds, synthesized in our laboratory. For the calculation of pIC_{50} (-log IC_{50}) values used in the QSAR analysis, the IC_{50} (μM) values were taken in molar range and then expressed in negative logarithmic units. The chemical structures and corresponding pIC_{50} values are listed in Table 1 (see SI). The set of compounds was divided into training and test sets. The test set compounds were selected by considering both the distribution of biological data and structural diversity of the molecules. Compound **16n** was used as a template due to its high tubulin binding activity.

Molecular docking. Molecular docking studies were performed as previously described in full detail.[41]

CoMFA and CoMSIA. Molecular docking studies were performed as previously described in full detail.[41] To generate 3D-QSAR models, the compounds were aligned to template compound **16n** on a backbone which is common among all structures to minimize the sum-of-squares deviation between reference backbone in each molecule and the corresponding core in the template.

Supporting Information Available: 1SA0_prepared.pdb**,** 1SA0.pdb; ID codes for compounds **15b (**M01.pdb), **15c (**M02.pdb), **15f (**M03.pdb), **15g** (M04.pdb), **15a (**M05.pdb), **16a (**M06.pdb), **16c (**M07.pdb), **16d** (M08.pdb), **16e** (M09.pdb), **16f** (M10.pdb), **16g (**M11.pdb), **16h** (M12.pdb), **16i** (M13.pdb), **16j** (M14.pdb), **16k** (M15.pdb), **16l** (M16.pdb), **16m** (M17.pdb), **16n** (M18.pdb), **16o** (M19.pdb); Authors will release the atomic coordinates and experimental data upon article publication.
Methodology of the panel screen; Visualization of z-scores for **16n**, **16o**; Cell cycle analysis data of K562 cells treated with **15b**, **15c**, **16c**, **16d**, **16o** and colchicine; ^{1}H- and ^{13}C-NMR spectra of compounds **15a-15h**, **16a-16p**, **17a-17b**, **18**, **and 19**; Molecular formula strings of all compounds.
This material is available free of charge via the Internet at http://pubs.acs

Author Information
Corresponding Author
*Phone: +49 251-8332195. Fax: +0049 251-8332144. E-mail: prinzh@uni-muenster.de

Acknowledgement
We wish to thank Angelika Zinner and Marina Wollmann for excellent technical assistance. Also, we would like to thank Sasidhar Maddula, Ilgin Yildiz, Maria Janzen and Maximilian Nunziante, a team at Oncolead GmbH involved in carrying out the profiling experiments in the cell line panel.

Abbreviations used

APCI: atmospheric pressure chemical ionization, CoMFA: comparative molecular field analysis, CoMSIA: comparative molecular similarity index analysis, EBI: N,N′-ethylene-bis(iodoacetamide), GOLD: Genetic Optimisation for Ligand Docking, ITP: inhibition of tubulin polymerization, MTP: microtubule protein, ND: not determined, SARs: structure−activity relationships, SI: supporting information, SRB: sulforhodamine B.

References

1. Nogales, E. Structural insights into microtubule function. *Annu. Rev. of Biochem.* **2000,** *69*, 277-302.

2. Honore, S.; Pasquier, E.; Braguer, D. Understanding microtubule dynamics for improved cancer therapy. *Cell. Mol. Life Sci.* **2005,** *62*, 3039-3056.

3. Pellegrini, F.; Budman, D. R. Review: tubulin function, action of antitubulin drugs, and new drug development. *Cancer Invest.* **2005,** *23*, 264-273.

4. Hadfield, J. A.; Ducki, S.; Hirst, N.; McGown, A. T. Tubulin and microtubules as targets for anticancer drugs. *Prog. Cell Cycle Res.* **2003,** *5*, 309-325.

5. Hearn, B. R.; Shaw, S. J.; Myles, D. C. Microtubule targeting agents. *Comprehensive Medicinal Chemistry II* **2007,** *7*, 81-110.

6. Li, Q.; Sham, H. L. Discovery and development of antimitotic agents that inhibit tubulin polymerisation for the treatment of cancer. *Expert Opin. Ther. Patents* **2002,** *12*, 1663-1702.

7. Kaur, R.; Kaur, G.; Gill, R. K.; Soni, R.; Bariwal, J. Recent developments in tubulin polymerization inhibitors: An overview. *Eur. J. Med. Chem.* **2014,** *87*, 89-124.

8. Jordan, M. A. Mechanism of action of antitumor drugs that interact with microtubules and tubulin. *Curr. Med. Chem. Anticancer Agents* **2002,** *2*, 1-17.

9. Mahindroo, N.; Liou, J. P.; Chang, J. Y.; Hsieh, H. P. Antitubulin agents for the treatment of cancer - a medicinal chemistry update. *Expert Opin. Ther. Patents* **2006,** *16*, 647-691.

10. Baldessarini, R. J. In *Goodman & Gilman´s The pharmacological basis of therapeutics*, 11th ed.; Brunton, L. L.; Lazo, J. S.; Parker, K. L., Eds. McGraw-Hill: New York, 2006; pp. 429-459.

11. Motohashi, N.; Gollapudi, S. R.; Emrani, J.; Bhattiprolu, K. R. Antitumor properties of phenothiazines. *Cancer Invest.* **1991,** *9*, 305-319.

12. Ohlow, M. J.; Moosmann, B. Phenothiazine: the seven lives of pharmacology´s first lead structure. *Drug Discovery Today,* **2011,** *16*, 119-131.

13. Prinz, H.; Chamasmani, B.; Vogel, K.; Böhm, K. J.; Aicher, B.; Gerlach, M.; Günther, E. G.; Amon, P.; Ivanov, I.; Müller, K. N-Benzoylated phenoxazines and phenothiazines: synthesis, antiproliferative activity, and inhibition of tubulin polymerization. *J. Med. Chem.* **2011,** *54*, 4247-4263.

14. Welsch, M. E.; Snyder, S. A.; Stockwell, B. R. Privileged scaffolds for library design and drug discovery. *Curr. Opin. Chem. Biol.* **2010,** *14*, 347-361.

15. Asif, M. Piperazine and pyrazine containing molecules and their diverse pharmacological activities. *IJASR* **2015,** *1*, 5-11.

16. Patel, R. V.; Park, S. W. An evolving role of piperazine moieties in drug design and discovery. *Mini Rev. Med. Chem.* **2013,** *13*, 1579-1601.

17. Baasner, S.; Emig, P.; Gerlach, M.; Müller, G.; Paulini, K.; Schmidt, P.; Burger, A. M.; Fiebig, H.-H.; Günther, E. G. D-82318 - A novel, synthetic, low molecular weight tubulin inhibitor with potent in vivo antitumor activity. *poster 112; EORTC-NCI-AACR meeting Frankfurt* **2002**.

18. Gerlach, M.; Claus, E.; Baasner, S.; Müller, G.; Polymeropoulos, E.; Schmidt, P.; Gunther, E.; Engel, J. Design and synthesis of a focused library of novel aryl- and heteroaryl-ketopiperazides. *Arch. Pharm. (Weinheim)* **2004,** *337*, 695-703.

19. Ishii, K.; Sugimura, Y. Identification of a new pharmacological activity of the phenylpiperazine derivative naftopidil: tubulin-binding drug. *J. Chem. Biol.* **2015,** *8*, 5-9.

20. Chopra, A.; Anderson, A.; Giardina, C. Novel Piperazine-based Compounds Inhibit Microtubule Dynamics and Sensitize Colon Cancer Cells to Tumor Necrosis Factor-induced Apoptosis. *J. Biol. Chem.* **2014,** *289*, 2978-2991.

21. Yin, Y.; Qiao, F.; Jiang, L. Y.; Wang, S. F.; Sha, S.; Wu, X.; Lv, P. C.; Zhu, H. L. Design, synthesis and biological evaluation of (*E*)-3-(3,4-dihydroxyphenyl)acrylylpiperazine derivatives as a new class of tubulin polymerization inhibitors. *Bioorg. Med. Chem.* **2014,** *22*, 4285-4292.

22. Eregowda, G. B.; Kalpana, H. N.; Hegde, R.; Thimmaiah, K. N. Synthesis and analysis of structural features of phenoxazine analogues needed to reverse vinblastine resistance in multidrug resistant (MDR) cancer cells. *Indian J. Chem.* **2000,** *39B*, 243-259.

23. Eastmond, G. C.; Gilchrist, T. L.; Paprotny, J.; Steiner, A. Cyano-activated fluoro displacement reactions in the synthesis of cyanophenoxazines and related compounds. *New J. Chem.* **2001,** *25*, 385-390.

24. Hernandez-Olmos, V.; Abdelrahman, A.; El-Tayeb, A.; Freudendahl, D.; Weinhausen, S.; Müller, C. E. N-Substituted phenoxazine and acridone derivatives: structure-activity relationships of potent P2X4 receptor antagonists. *J. Med. Chem.* **2012,** *55*, 9576-9588.

25. Marcu, A.; Schurigt, U.; Müller, K.; Moll, H.; Krauth-Siegel, R. L.; Prinz, H. Inhibitory effect of phenothiazine- and phenoxazine-derived chloroacetamides on Leishmania major growth and Trypanosoma brucei trypanothione reductase. *Eur. J. Med. Chem.* **2016,** *108*, 436-443.

26. Lozzio, C. B.; Lozzio, B. B. Human chronic myelogenous leukemia cell-line with positive philadelphia chromosome. *Blood* **1975,** *45*, 321-334.

27. Moon, E. Y.; Lerner, A. Benzylamide sulindac analogues induce changes in cell shape, loss of microtubules and G(2)-M arrest in a chronic lymphocytic leukemia (CLL) cell line and apoptosis in primary CLL cells. *Cancer Res.* **2002,** *62*, 5711-5719.

28. Prinz, H.; Ishii, Y.; Hirano, T.; Stoiber, T.; Camacho Gomez, J. A.; Schmidt, P.; Düssmann, H.; Burger, A. M.; Prehn, J. H.; Günther, E. G.; Unger, E.; Umezawa, K. Novel benzylidene-9(10*H*)-anthracenones as highly active antimicrotubule agents. Synthesis, antiproliferative activity, and inhibition of tubulin polymerization. *J. Med. Chem.* **2003,** *46*, 3382-3394.

29. Fleming, F. F.; Yao, L. H.; Ravikumar, P. C.; Funk, L.; Shook, B. C. Nitrile-containing pharmaceuticals: efficacious roles of the nitrile pharmacophore. *J. Med. Chem.* **2010,** *53*, 7902-7917.

30. Sharma, S. V.; Haber, D. A.; Settleman, J. Cell line-based platforms to evaluate the therapeutic efficacy of candidate anticancer agents. *Nat. Rev. Cancer* **2010,** *10*, 241-253.

31. Paull, K. D.; Shoemaker, R. H.; Hodes, L.; Monks, a.; Scudiero, D. a.; Rubinstein, L.; Plowman, J.; Boyd, M. R. Display and Analysis of Patterns of Differential Activity of Drugs against Human-Tumor Cell-Lines - Development of Mean Graph and Compare Algorithm. *J. Natl. Cancer Inst.* **1989,** *81*, 1088-1092.

32. Bøyum, A. Isolation of mononuclear cells and granulocytes from human blood - Isolation of mononuclear cells by one centrifugation and of granulocytes by combining centrifugation and sedimentation at 1 G. *Scand. J. Clin. Lab. Inv.* **1968,** *S 21*, 77-89.

33. Gaskin, F.; Cantor, C. R.; Shelanski, M. L. Turbidimetric studies of the in vitro assembly and disassembly of porcine neurotubules. *J. Mol. Biol.* **1974,** *89*, 737-755.

34. Prota, A. E.; Bargsten, K.; Diaz, J. F.; Marsh, M.; Cuevas, C.; Liniger, M.; Neuhaus, C.; Andreu, J. M.; Altmann, K. H.; Steinmetz, M. O. A new tubulin-binding site and pharmacophore for microtubule-destabilizing anticancer drugs. *Proc. Natl. Acad. Sci. U. S. A.* **2014,** *111*, 13817-13821.

35. Canela, M. D.; Perez-Perez, M. J.; Noppen, S.; Saez-Calvo, G.; Diaz, J. F.; Camarasa, M. J.; Liekens, S.; Priego, E. M. Novel colchicine-site binders with a cyclohexanedione scaffold identified through a ligand-based virtual screening approach. *J. Med. Chem.* **2014,** *57*, 3924-3938.

36. Cao, D.; Liu, Y. B.; Yan, W.; Wang, C. Y.; Bai, P.; Wang, T. J.; Tang, M. H.; Wang, X. Y.; Yang, Z.; Ma, B. Y.; Ma, L.; Lei, L.; Wang, F.; Xu, B. X.; Zhou, Y. Y.; Yang, T.; Chen, L. J. Design, synthesis, and evaluation of in vitro and in vivo anticancer activity of 4-substituted coumarins: a novel class of potent tubulin polymerization inhibitors. *J. Med. Chem.* **2016,** *59*, 5721-5739.

37. Fortin, S.; Lacroix, J.; Cote, M. F.; Moreau, E.; Petitclerc, E.; Gaudreault, R. C. Quick and simple detection technique to assess the binding of antimicrotubule agents to the colchicine-binding site. *Biol. Proced. Online* **2010,** *12*, 113-117.

38. Kanthou, C.; Greco, O.; Stratford, A.; Cook, I.; Knight, R.; Benzakour, O.; Tozer, G. The tubulin-binding agent combretastatin A-4-phosphate arrests endothelial cells in mitosis and induces mitotic cell death. *Am. J. Pathol.* **2004,** *165*, 1401-1411.

39. Simoni, D.; Grisolia, G.; Giannini, G.; Roberti, M.; Rondanin, R.; Piccagli, L.; Baruchello, R.; Rossi, M.; Romagnoli, R.; Invidiata, F. P.; Grimaudo, S.; Jung, M. K.; Hamel, E.; Gebbia, N.; Crosta, L.; Abbadessa, V.; Di Cristina, A.; Dusonchet, L.; Meli, M.; Tolomeo, M. Heterocyclic and phenyl double-bond-locked combretastatin analogues possessing potent apoptosis-inducing activity in HL60 and in MDR cell lines. *J. Med. Chem.* **2005,** *48*, 723-36.

40. Fortin, S.; Wei, L. H.; Moreau, E.; Lacroix, J.; Cote, M. F.; Petitclerc, E.; Kotra, L. P.; C-Gaudreault, R. Design, synthesis, biological evaluation, and structure-activity relationships of substituted phenyl 4-(2-oxoimidazolidin-1-yl)-benzenesulfonates as new tubulin inhibitors mimicking combretastatin A-4. *J. Med. Chem.* **2011,** *54*, 4559-4580.

41. Ghasemi, J. B.; Aghaee, E.; Jabbari, A. Docking, CoMFA and CoMSIA studies of a series of N-benzoylated phenoxazines and phenothiazines derivatives as antiproliferative agents. *Bull. Korean Chem. Soc.* **2013,** *34*, 899-906.

42. Yang, X. H.; Wen, Q.; Zhao, T. T.; Sun, J.; Li, X.; Xing, M.; Lu, X.; Zhu, H. L. Synthesis, biological evaluation, and molecular docking studies of cinnamic acyl 1,3,4-thiadiazole amide derivatives as novel antitubulin agents. *Bioorgan. Med. Chem.* **2012,** *20*, 1181-1187.

43. Cramer, R. D.; Patterson, D. E.; Bunce, J. D. Comparative molecular-field analysis (Comfa). 1. Effect of shape on binding of steroids to carrier proteins. *J. Am. Chem. Soc.* **1988,** *110*, 5959-5967.

44. Ghasemi, J. B.; Pirhadi, S.; Ayati, M. 3D-QSAR studies of 2-arylbenzoxazoles as novel cholesteryl ester transfer protein inhibitors. *Bull. Korean Chem. Soc.* **2011,** *32*, 645-650.

45. Klebe, G.; Abraham, U.; Mietzner, T. Molecular similarity indexes in a comparative-analysis (Comsia) of drug molecules to correlate and predict their biological activity. *J. Med. Chem.* **1994,** *37*, 4130-4146.

46. Thimmaiah, K. N.; Easton, J. B.; Germain, G. S.; Morton, C. L.; Kamath, S.; Buolamwini, J. K.; Houghton, P. J. Identification of N10-substituted phenoxazines as potent and specific inhibitors of Akt signaling. *J. Biol. Chem.* **2005,** *280*, 31924-31935.

47. Müller, K.; Leukel, P.; Ziereis, K.; Gawlik, I. Antipsoriatic anthrones with modulated redox properties. 2. Novel derivatives of chrysarobin and isochrysarobin — antiproliferative activity and 5-lipoxygenase inhibition. *J. Med. Chem.* **1994,** *37*, 1660-1669.

Table 1. Antiproliferative activity of phenothiazine derivatives **15a-15h** and reference compounds against K562 cells and inhibition of tubulin polymerization.

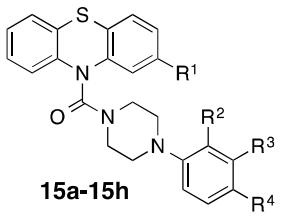

15a-15h

cmpd	R^1	R^2	R^3	R^4	K562 IC_{50}[a] [μM]	ITP IC_{50}[b] [μM]
15a	H	H	H	H	0.13	0.81 ± 0.14
15b	H	OCH_3	H	H	0.02	0.60
15c	H	H	OCH_3	H	0.02	0.55
15d	H	H	H	OCH_3	3.70	ND
15e	H	H	H	CN	0.39	ND
15f	Cl	OCH_3	H	H	0.09	0.51
15g	Cl	H	OCH_3	H	0.03	0.92
15h	Cl	H	H	OCH_3	1.90	>10
colchicine					0.02	1.4
nocodazole					ND	0.76
podophyllotoxin					ND	0.35
vinblastine sulphate					0.001	0.13
adriamycin					0.01	ND

[a] IC_{50}, concentration of compound required for 50% inhibition of cell growth (K562). Cells were treated with drugs for 48 h. IC_{50} values are the means of at least three independent determinations (SD < 10%). [b] ITP = inhibition of tubulin polymerization; IC_{50} values represent the compound concentration at which the maximum of tubulin assembly level amounts 50% of the level of the control without the compound (determined after 45 min polymerization of tubulin at 37°C).

Table 2. Antiproliferative activity of phenoxazine derivatives **16a-16p** gainst K562 cells and and inhibition of tubulin polymerization.

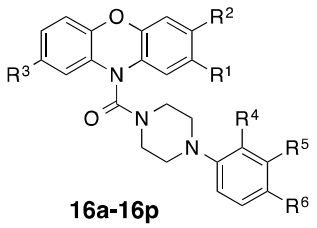

16a-16p

cmpd	R^1	R^2	R^3	R^4	R^5	R^6	K562 $IC_{50}{}^a$ [μM]	ITP $IC_{50}{}^b$ [μM]
16a	H	H	H	H	H	H	0.03	1.38
16b	H	H	H	H	H	CH_3	1.39	ND
16c	H	H	H	OCH_3	H	H	0.02	0.64
16d	H	H	H	H	OCH_3	H	0.02	0.69
16e	H	H	H	H	H	OCH_3	3.13	14.3
16f	H	H	H	H	H	Cl	0.63	0.83
16g	H	H	H	H	H	CF_3	> 60	> 10
16h	H	H	H	H	H	NO_2	> 70	> 10
16i	H	H	H	H	H	CN	> 20	> 10
16j	Cl	H	H	OCH_3	H	H	0.03	0.62
16k	Cl	H	H	H	OCH_3	H	0.03	0.80
16l	Cl	H	Cl	OCH_3	H	H	0.13	1.19
16m	Cl	H	Cl	H	OCH_3	H	0.18	0.90
16n	H	CN	H	OCH_3	H	H	0.03	0.32
16o	H	CN	H	H	OCH_3	H	0.007	0.36
16p	H	CN	H	H	H	OCH_3	0.21	3.38

[a, b] For details see Table I.

48

Table 3. Antiproliferative activities of structurally related analogs against K562 cells and and inhibition of tubulin polymerization.

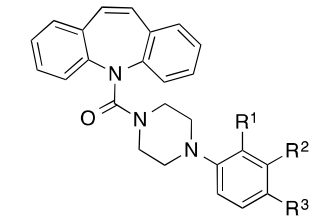

17a, $R^1 = OCH_3$, $R^2 = R^3 = H$
17b, $R^2 = OCH_3$, $R^1 = R^3 = H$

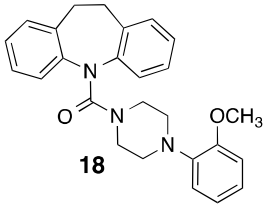

18

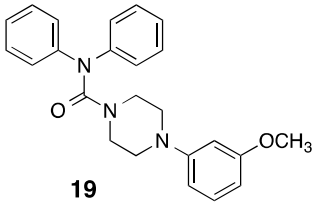

19

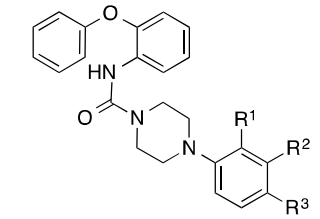

20a, $R^1 = OCH_3$, $R^2 = R^3 = H$
20b, $R^1 = H$, $R^2 = OCH_3$, $R^3 = H$
20c, $R^1 = R^2 = H$, $R^3 = OCH_3$

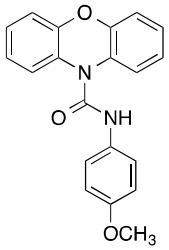

21

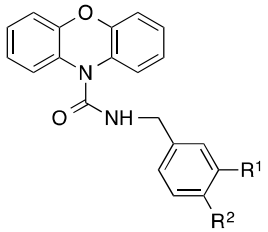

22a, $R^1 = OCH_3$, $R^2 = H$
22b, $R^1 = H$, $R^2 = OCH_3$

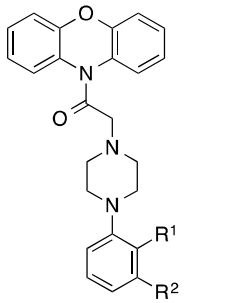

24a, $R^1 = OCH_3$, $R^2 = H$
24b, $R^1 = H$, $R^2 = OCH_3$

cmpd	K562 IC_{50}[a] [μM]	ITP IC_{50}[b] [μM]	cmpd	K562 IC_{50}[a] [μM]	ITP IC_{50}[b] [μM]
3a	16.80	ND	**20a**	> 10	> 10
17a	0.45	2.83	**20b**	> 10	> 10
17b	0.94	3.56	**20c**	> 10	> 10
18	0.84	10.73	**22a**	6	8.53
19	18	> 10	**22b**	19	9
21	> 80	> 10	**24a**	9	> 10
			24b	5	> 10

[a, b] For details see Table I.

Table 4. The most sensitive and resistant cell lines after treatment of solid tumor cell lines with **16o**

cmpd	**16o**	
number of tested cell lines	94	
Maximum concentration [μM]	10	
Mimimum concentration [μM]	0.0001	
Activity (using log transformed data)	**GI_{50} [μM]**	
Maximum	0.0079	
Minimum	0.0014	
Mean	0.0033	
Median	0.0032	
Most sensitive cell lines (8 shown)	**GI_{50} [μM]**	**zScore**[a]
SKNAS	0.0014	-1,8940
SKBR3	0.0015	-1,8062
MG63	0.0015	-1,7161
NCIH82	0.0016	-1,6430
IMR90	0.0016	-1,6172
RD	0.0017	-1,5359
PANC1005	0.0017	-1,5322
JAR	0.0017	-1,4857
Most resistant cell lines (8 shown)	**GI_{50} [μM]**	**zScore**[a]
CACO2	0.0079	1,9235
CLS439	0.0078	1,9019
COLO678	0.0075	1,8268
NCIH292	0.0067	1,5611
PANC1	0.0065	1,5159
HT29	0.0064	1,4760
JIMT1	0.0059	1,2806
SKLMS1	0.0059	1,2802

[a]See Supporting Information for visualization of zScores

Figure Legends

Scheme 1 Reagents and conditions: (a) bis(trichloromethyl) carbonate, 1,2-dichloroethane, pyridine, 75 °C, 3 h; (b) appropriate 1-phenylpiperazine, reflux, TLC control; (c) appropriate aniline or benzylamine, reflux, 2h.

Scheme 2 Reagents and conditions: (a) chloroacetyl chloride, toluene, 90 °C, N_2; (b) appropriate 1-phenylpiperazine, reflux, TLC control.

Scheme 3 (a) bis(trichloromethyl) carbonate, 1,2-dichloroethane, pyridine, 75 °C, 1 h, N_2, appropriate 1-phenylpiperazine, reflux, 2 h; b) benzoyl chloride, 1,2-dichloroethane, triethylamine, reflux, 3h.

Chart 1 Phenothiazine (**1a)**, Chlorpromazin (**2**), Phenoxazine **(3a**), and 10-(3-Hydroxy-4-methoxybenzoyl)-10*H*-phenoxazine-3-carbonitrile (**4**).

Chart 2 Phenylpiperazine-based inhibitors of tubulin polymerization.

Figure 1 **A**, Visual display of the most sensitive and most resistant cell lines (8 are shown each) from the panel screening by using the z-score. Activities against resting PBMC were > 10 μM. The mean concentration required to inhibit 50% of the growth for all cell lines (GI_{50}) is defined as zero value. Horizontal bars represent the relative difference in the GI_{50} values, expressed as z-score. Bars oriented to the right (positive z-scores) indicate lower sensitivity to **16o** treatment; bars oriented to the left (negative z-scores) indicate higher sensitivity to **16o** treatment; **B,** box-and-whisker diagram.

Figure 2 **A**, Polymerization curves of tubulin (in total 1.2 mg/mL protein; ~85 % tubulin plus ~15% microtubule-associated proteins) at 37 °C by various concentrations of **16o**; turbidity was recorded at 360 nm. The steady-state tubulin assembly level in the absence of inhibitor was set 100%. **B**, IC_{50} values, representing the concentration for 50% inhibition of the maximum tubulin polymerization level, were determined by sigmoidal fitting the plot of the steady state levels of tubulin assembly (taken after 45 min) against drug concentration.

Figure 3 Inhibition of EBI binding to β-tubulin by **15b** and **16o** and**.** K562 cells were treated with DMSO, colchicine (5 μM), vinblastine (5 μM), **15b** (20 or 40 μM) or **16o** (14 or 7 μM) for 2h. Next, (EBI, 100 μM) was added, and after 1.5 h, the cells were harvested and cell extracts were prepared for Western blot analysis using an anti-β-tubulin antibody. EBI cross-links cysteine residues in β-tubulin, resulting in the formation of a β-tubulin adduct (second immunoreactive band) that migrates faster than β-tubulin. The formation of the EBI/β-tubulin adduct is prevented by compounds that preoccupy to the colchicine-binding site in β-tubulin.

Figure 4 Induction of cell cycle arrest by **16o**. **A**, Cell cycle distribution of K562 cells showing the effect of 24 h-treatment with **16o (A)** and colchicine (**B)** (24 h assay). K562 cells were untreated, treated with different concentrations of **16o.** After treatment the cells were collected and cell cycle distribution was measured by flow cytometry with a FACSCalibur (Becton Dickinson), Software CellQuest Pro Version 5.2.

Figure 5 SAR summary

Figure 6 The best docked conformation of the most potent tubulin polymerization inhibitor (**16n**) in the binding site of tubulin results two hydrogen bonds, π-cation and π - sigma interactions.

Figure 7 Observed against predicted activities for the training and test sets of compounds based on CoMFA-RF model.

Figure 8 CoMFA contour map displaying steric (a) and electrostatic (b) fields in combination with compound **16n**. Green contours show contribution for sterically favorable interactions with the receptor and yellow contours show sterically unfavorable regions, while blue and red contours show electropositive and electronegative charge favorable regions, respectively.

Figure 9 CoMSIA contour map displaying steric (a), electrostatic (b), hydrogen bond acceptor (c) and hydrophobic (d) fields in combination with compound **16n**. Based on steric contour map, green and yellow contours show contribution for sterically favorable and unfavorable interactions with the receptor, respectively, while blue and red contours in electrostatic fields show electropositive and electronegative charge favorable regions, respectively. In the hydrophobic contour map, yellow and white regions indicate the areas where hydrophobic and hydrophilic properties are preferred, respectively, while in hydrogen bond acceptor field, magenta contours show regions where hydrogen bond acceptor groups are favored and red contours indicate regions where hydrogen bond acceptor groups are unfavorable.

53

Fig. 1

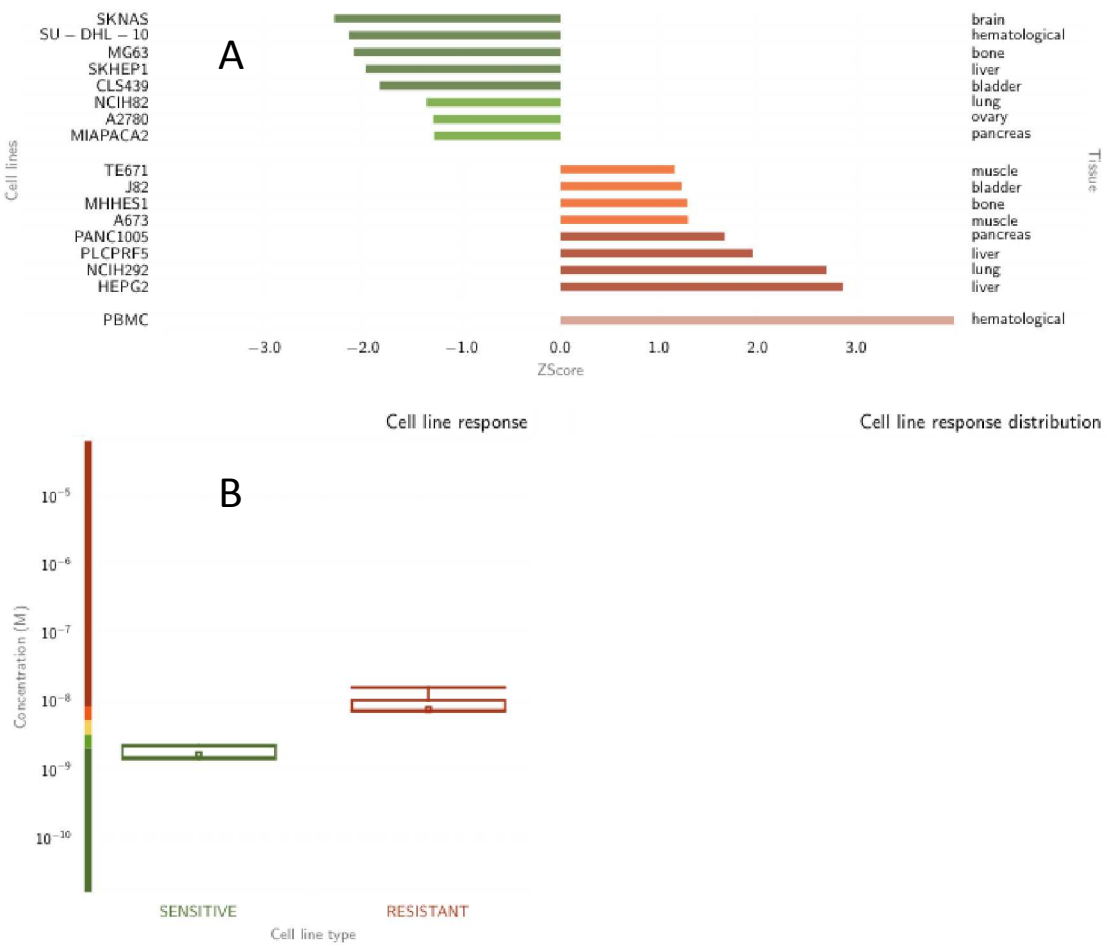
A
SKNAS
SU – DHL – 10
MG63
SKHEP1
CLS439
NCIH82
A2780
MIAPACA2
TE671
J82
MHHES1
A673
PANC1005
PLCPRF5
NCIH292
HEPG2
PBMC
Cell lines
brain
hematological
bone
liver
bladder
lung
ovary
pancreas
muscle
bladder
bone
muscle
pancreas
liver
lung
liver
hematological
Tissue
−3.0
−2.0
−1.0
0.0
1.0
2.0
3.0
ZScore
Cell line response
Cell line response distribution
B
Concentration (M)
SENSITIVE
RESISTANT
Cell line type

54

Fig. 2

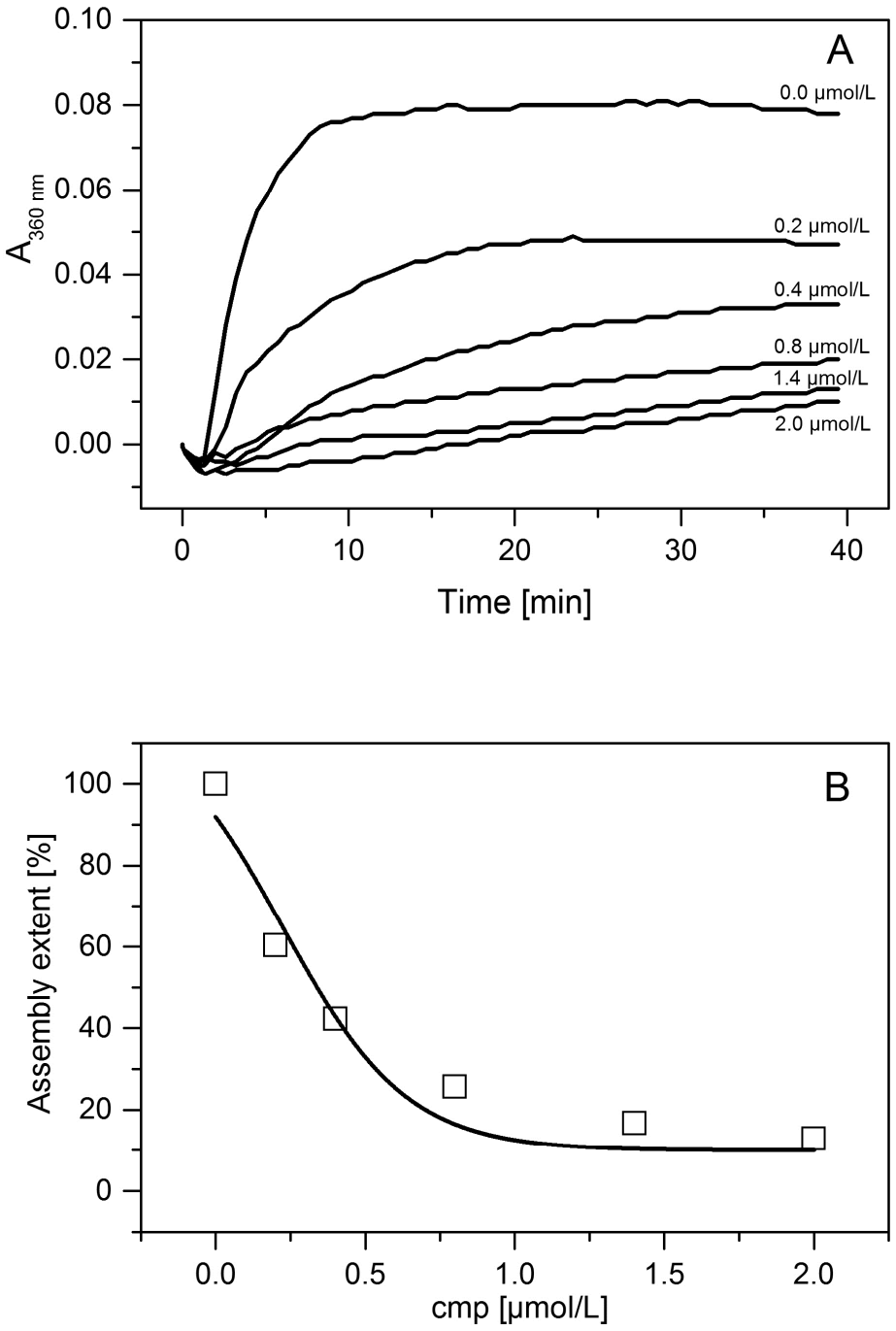
A
0.0 µmol/L
0.2 µmol/L
0.4 µmol/L
0.8 µmol/L
1.4 µmol/L
2.0 µmol/L
$A_{360\ nm}$
0.10
0.08
0.06
0.04
0.02
0.00
0
10
20
30
40
Time [min]
B
Assembly extent [%]
100
80
60
40
20
0
0.0
0.5
1.0
1.5
2.0
cmp [µmol/L]

55

Fig. 3

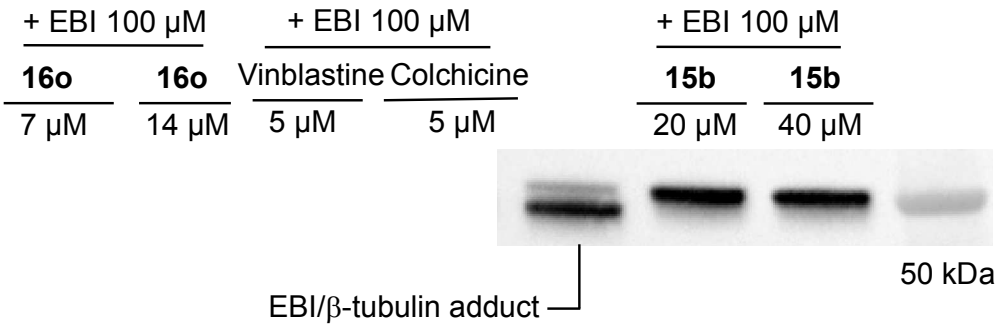
+ EBI 100 μM
16o
7 μM
16o
14 μM
+ EBI 100 μM
Vinblastine
5 μM
Colchicine
5 μM
+ EBI 100 μM
15b
20 μM
15b
40 μM
50 kDa
EBI/β-tubulin adduct

56

Fig. 4

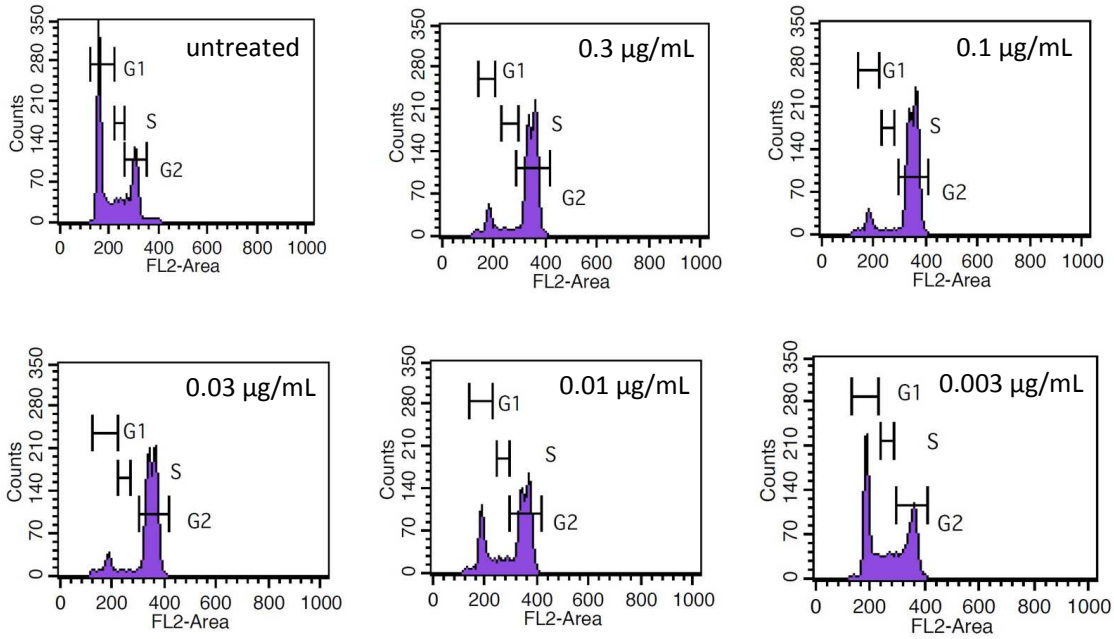
untreated
0.3 µg/mL
0.1 µg/mL
0.03 µg/mL
0.01 µg/mL
0.003 µg/mL
G1
S
G2
Counts
FL2-Area
0
70
140
210
280
350
200
400
600
800
1000

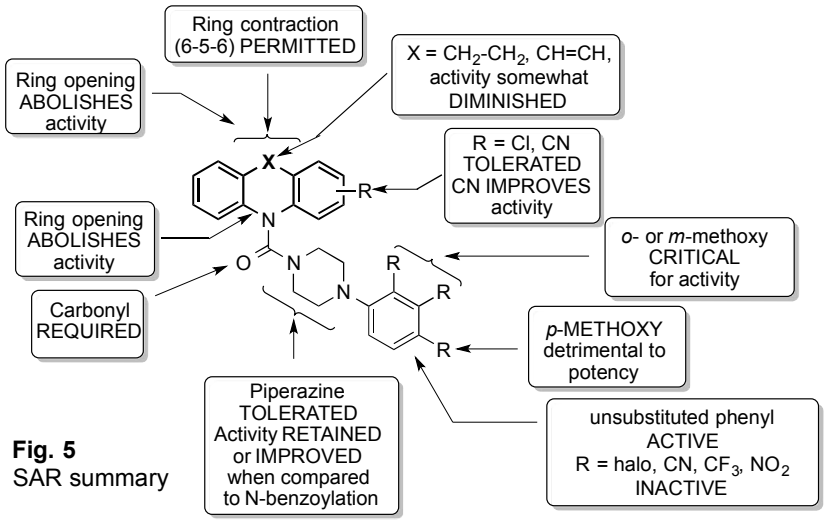

Fig. 5
SAR summary

58

Fig. 6

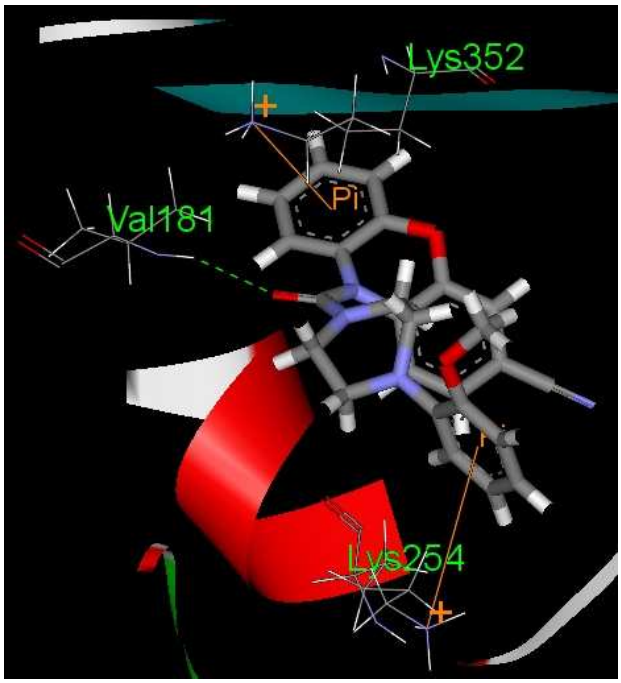

Fig. 7

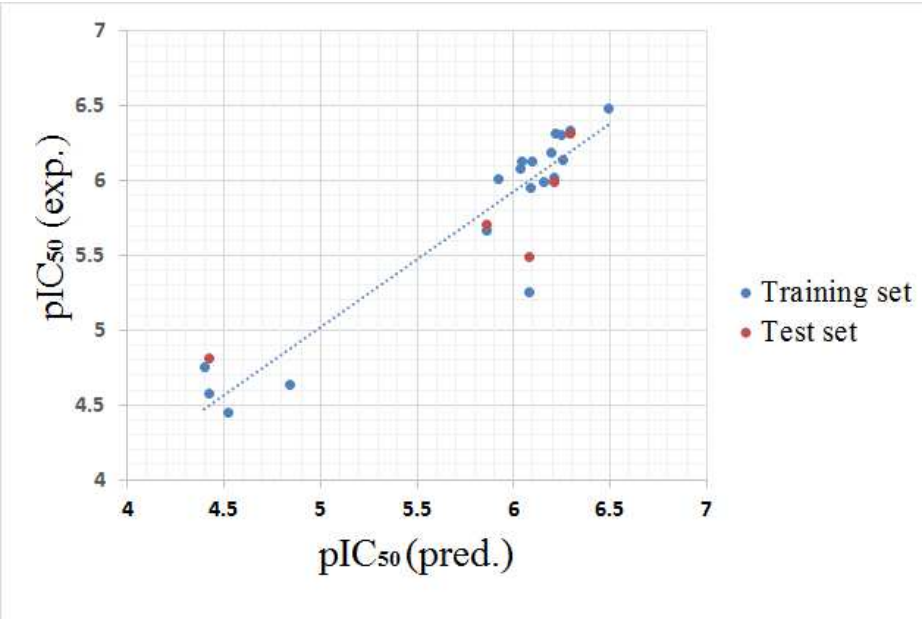
7
6.5
6
5.5
5
4.5
4
4
4.5
5
5.5
6
6.5
7
pIC50 (exp.)
pIC50 (pred.)
Training set
Test set

60

Fig. 8

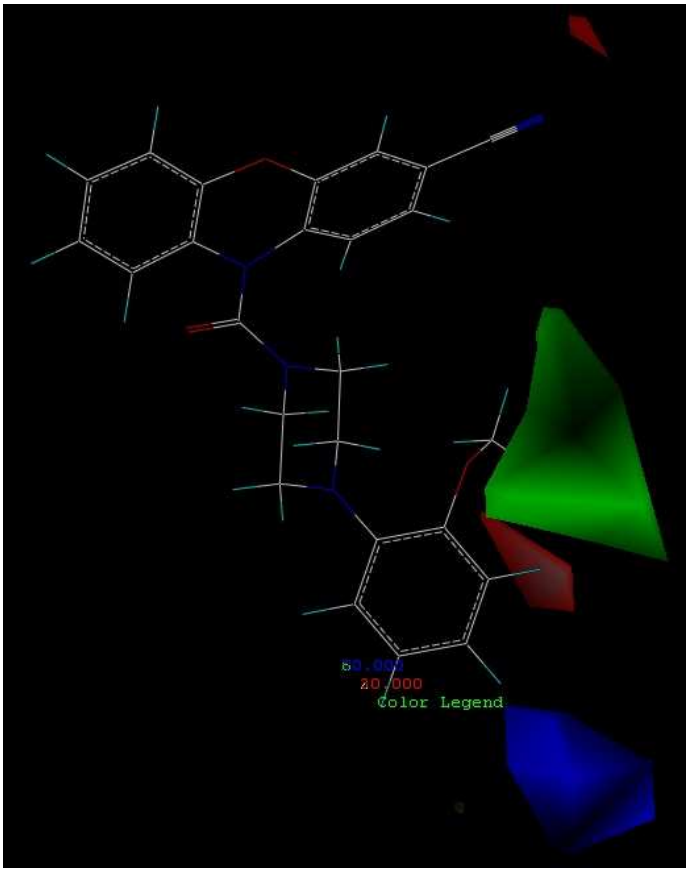

61

Fig. 9

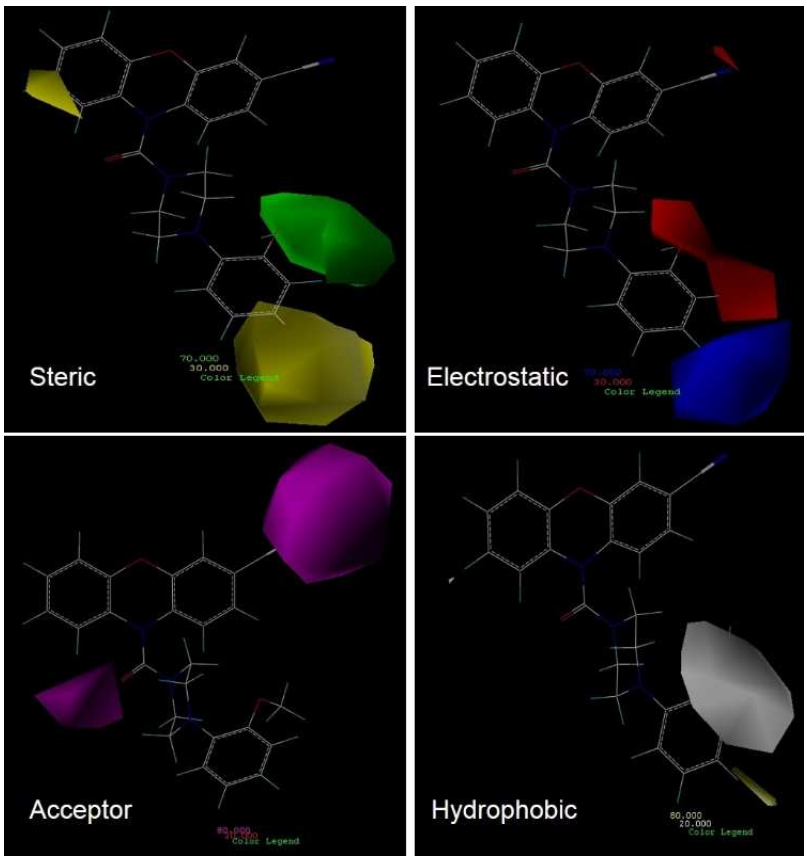

62

Chart 1

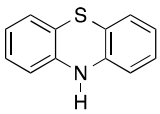

1a

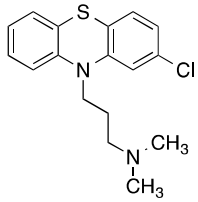

2, chlorpromazine

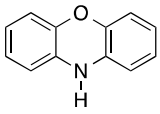

3a

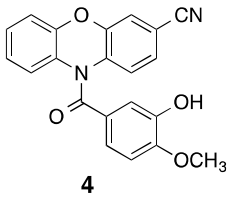

4

Chart 2

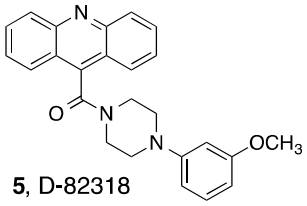

5, D-82318

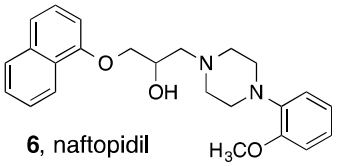

6, naftopidil

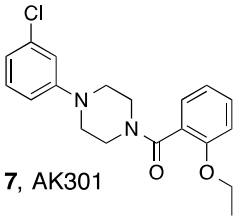

7, AK301

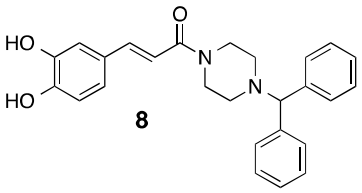

8

64

Chart 3

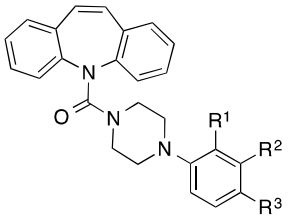

17a, $R^1 = OCH_3$, $R^2 = R^3 = H$
17b, $R^2 = OCH_3$, $R^1 = R^3 = H$

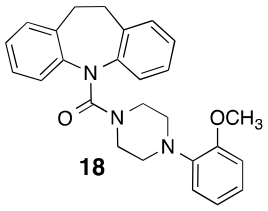

18

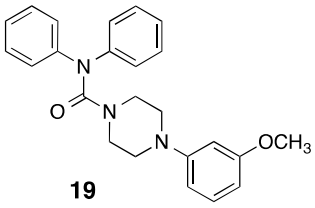

19

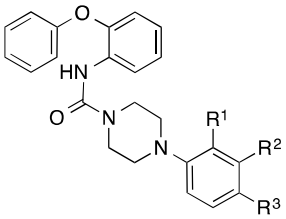

20a, $R^1 = OCH_3$, $R^2 = R^3 = H$
20b, $R^1 = H$, $R^2 = OCH_3$, $R^3 = H$
20c, $R^1 = R^2 = H$, $R^3 = OCH_3$

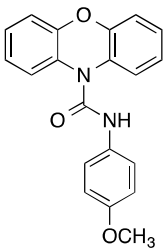

21

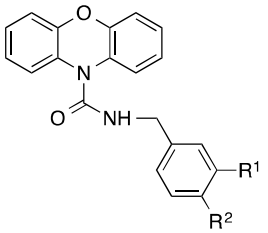

22a, $R^1 = OCH_3$, $R^2 = H$
22b, $R^1 = H$, $R^2 = OCH_3$

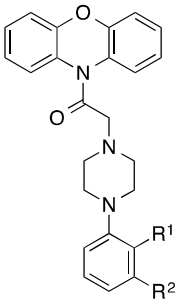

24a, $R^1 = OCH_3$, $R^2 = H$
24b, $R^1 = H$, $R^2 = OCH_3$

a

65

Scheme 1

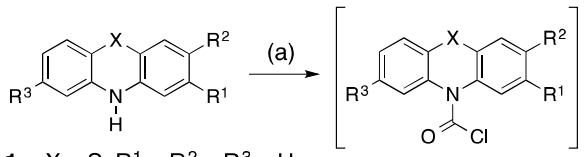

1a, X = S, $R^1 = R^2 = R^3 = H$
1b, X = S, $R^1 = Cl$, $R^2 = R^3 = H$
3a, X = O, $R^1 = R^2 = R^3 =$ H
3b, X = O, $R^1 = Cl$, $R^2 = R^3 = H$
3c, X = O, $R^1 = R^3 = Cl$, $R^2 = H$
3d, X = O, $R^1 = R^3 = H$, $R^2 = CN$
9, X = CH=CH, $R^1 = R^2 = R^3 = H$
10, X = CH_2–CH_2, $R^1 = R^2 = R^3 = H$
11, X = C=O, $R^1 = R^2 = R^3 = H$

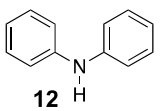
12

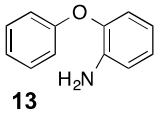
13

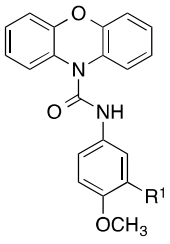
21

or

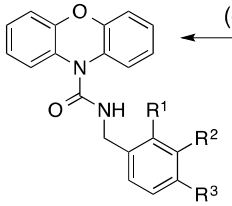

(c)

22a, $R^1 = R^3 = H$, $R^2 = OCH_3$
22b, $R^1 = R^2 = H$, $R^3 = OCH_3$

15a, X = S, $R^1 = R^2 = R^3 = R^4 = R^5 = R^6 = H$
15b, X = S, $R^1 = R^2 = R^3 = H$, $R^4 = OCH_3$, $R^5 = R^6 = H$
15c, X = S, $R^1 = R^2 = R^3 = R^4 = H$, $R^5 = OCH_3$, $R^6 = H$
15d, X = S, $R^1 = R^2 = R^3 = R^4 = R^5 = H$, $R^6 = OCH_3$
15e, X = S, $R^1 = R^2 = R^3 = R^4 = R^5 = H$, $R^6 = CN$
15f, X = S, $R^1 = Cl$, $R^2 = R^3 = H$, $R^4 = OCH_3$, $R^5 = R^6 = H$
15g, X = S, $R^1 = Cl$, $R^2 = R^3 = R^4 = H$, $R^5 = OCH_3$, $R^6 = H$
15h, X = S, $R^1 = Cl$, $R^2 = R^3 = R^4 = R^5 = H$, $R^6 = OCH_3$

16a, X = O, $R^1 = R^2 = R^3 = R^4 = R^5 = R^6 = H$
16b, X = O, $R^1 = R^2 = R^3 = R^4 = R^5 = H$, $R^6 = CH_3$
16c, X = O, $R^1 = R^2 = R^3 = H$, $R^4 = OCH_3$, $R^5 = R^6 = H$
16d, X = O, $R^1 = R^2 = R^3 = R^4 = H$, $R^5 = OCH_3$, $R^6 = H$
16e, X = O, $R^1 = R^2 = R^3 = R^4 = R^5 = H$, $R^6 = OCH_3$
16f, X = O, $R^1 = R^2 = R^3 = R^4 = R^5 = H$, $R^6 = Cl$
16g, X = O, $R^1 = R^2 = R^3 = R^4 = R^5 = H$, $R^6 = CF_3$
16h, X = O, $R^1 = R^2 = R^3 = R^4 = R^5 = H$, $R^6 = NO_2$
16i, X = O, $R^1 = R^2 = R^3 = R^4 = R^5 = H$, $R^6 = CN$
16j, X = O, $R^1 = Cl$, $R^2 = R^3 = H$, $R^4 = OCH_3$, $R^5 = H$, $R^6 = H$
16k, X = O, $R^1 = Cl$, $R^2 = R^3 = R^4 = H$, $R^5 = OCH_3$, $R^6 = H$
16l, X = O, $R^1 = Cl$, $R^2 = H$, $R^3 = Cl$, $R^4 = OCH_3$, $R^5 = R^6 =$ H
16m, X = O, $R^1 = Cl$, $R^2 = H$, $R^3 = Cl$, $R^4 = H$, $R^5 = OCH_3$, $R^6 = H$
16n, X = O, $R^1 = H$, $R^2 = CN$, $R^3 = H$, $R^4 = OCH_3$, $R^5 = R^6 = H$
16o, X = O, $R^1 = H$, $R^2 = CN$, $R^3 = R^4 = H$, $R^5 = OCH_3$, $R^6 = H$
16p, X = O, $R^1 = H$, $R^2 = CN$, $R^3 = R^4 = R^5 = H$, $R^6 = OCH_3$
17a, X = CH=CH, $R^1 = R^2 = R^3 = H$, $R^4 = OCH_3$, $R^5 = R^6 = H$
17b, X = CH=CH, $R^1 = R^2 = R^3 = R^4 = H$, $R^5 = OCH_3$, $R^6 = H$
18, X = CH_2–CH_2, $R^1 = R^2 = R^3 = H$, $R^4 = OCH_3$, $R^5 = R^6 = H$

66

Scheme 2

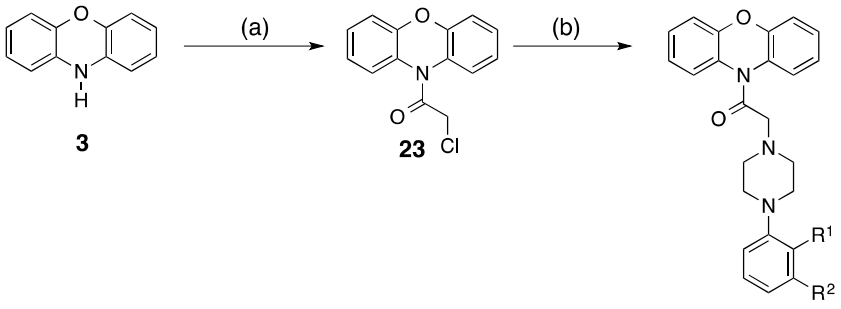

24a, $R^1 = OCH_3$, $R^2 = H$
24b, $R^1 = H$, $R^2 = OCH_3$,

Scheme 3

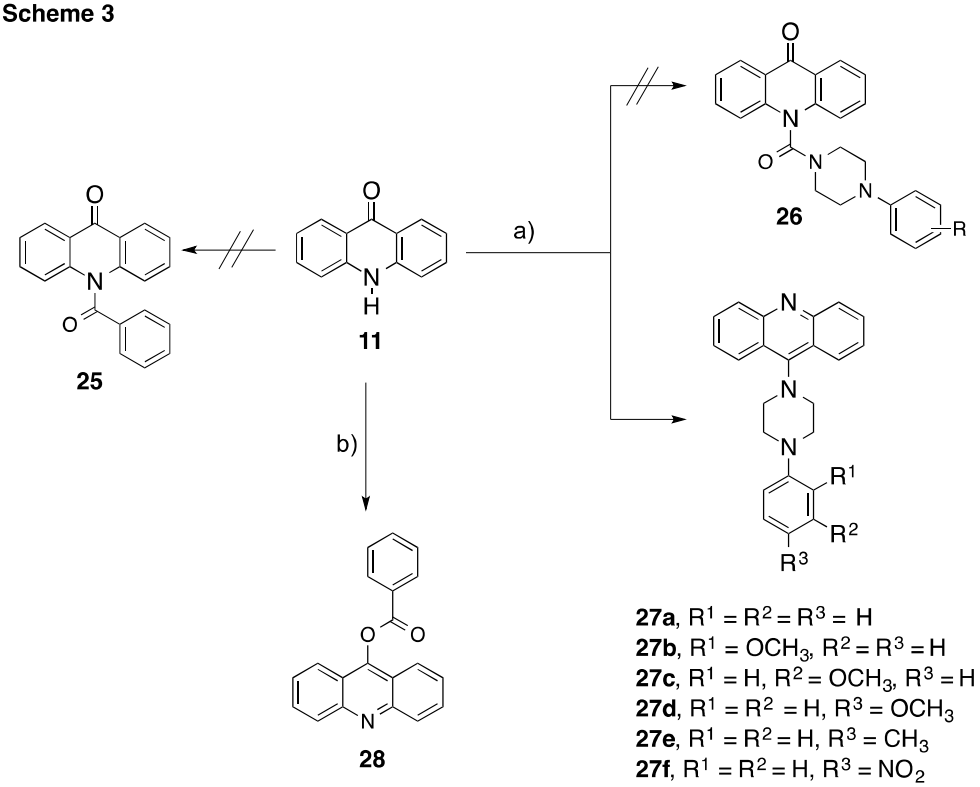

27a, $R^1 = R^2 = R^3 = H$
27b, $R^1 = OCH_3$, $R^2 = R^3 = H$
27c, $R^1 = H$, $R^2 = OCH_3$, $R^3 = H$
27d, $R^1 = R^2 = H$, $R^3 = OCH_3$
27e, $R^1 = R^2 = H$, $R^3 = CH_3$
27f, $R^1 = R^2 = H$, $R^3 = NO_2$

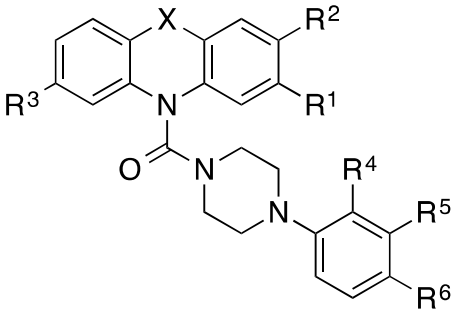

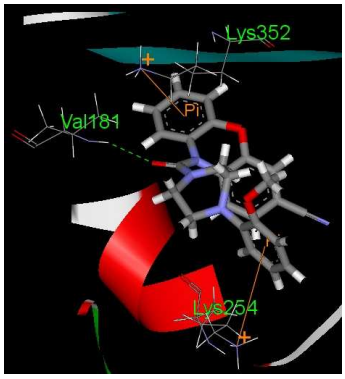

X = S, O, CH=CH, CH2–CH2

Table of Contents Graphic
Prinz et al.

Fig. 3

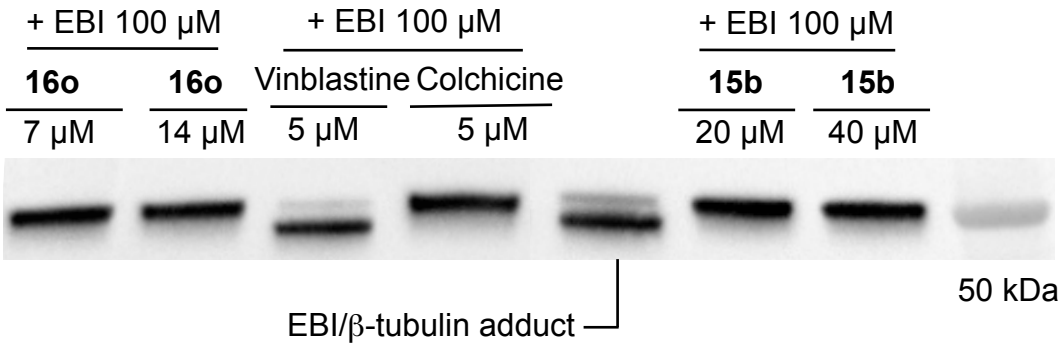
+ EBI 100 μM
+ EBI 100 μM
+ EBI 100 μM
16o
16o
Vinblastine
Colchicine
15b
15b
7 μM
14 μM
5 μM
5 μM
20 μM
40 μM
50 kDa
EBI/β-tubulin adduct